MULTISCALE MODELING OF POLYMER MEMBRANES FOR SOLDIERS PROTECTIVE CLOTHING

Jan Andzelm*, James Sloan, Eugene Napadensky, Rick Beyer, James Snyder, Steven McKnight
Weapons and materials Research Directorate, US Army Research Laboratory
Aberdeen Proving Ground, MD 21005-5069

Peter W. Chung
AMSRD-CI-HC, US Army Research Laboratory
Aberdeen Proving Ground, MD 21005-5069

ABSTRACT

The development of protective and breathable clothing is a very important goal set for the Future Force. Recently, a new polymer membrane made of an ionic triblock (A-B-A) copolymer was developed at the U.S. Army Research Laboratory (ARL) that provides an excellent selective barrier for soldier's protective clothing. We have used multiscale modeling to gain an understanding of the static and dynamic properties of this polymer membrane at detailed atomistic and mesoscale levels. These simulations lead to the prediction of the architecture and morphology of the membrane. We have also studied mesoscale morphology of the copolymer constrained by a surface or the nanopore. Mechanical properties of copolymer were calculated using the self-consistent homogenization theory.

1. INTRODUCTION

Currently, soldiers use mainly butyl rubber –based protective clothing. Such clothing protects soldier from chemical agents but it also prevents water permeability causing a high level of heat stress for the soldier. The new ARL polymer membrane (Crawford et al., 2001) is lightweight, flexible and can protect soldiers from chemical agents while improving soldier comfort because of high water permeability. This membrane, made of highly sulfonated poly(styrene-isobutylene-styrene) (sSIBS) is composed of a flexible elastic but low permeability barrier material (polyisobutylene, PI) and a breathable, hydrophilic component (sulfonated polystyrene, sPS). The thermodynamic immiscibility of the two components causes microphase separation, leading to complicated nanometer scale morphologies such as cylinders or lamellae. The sPS phase can form interconnected domains through the polymer and exhibits high selectivity for water, where selectivity is defined as the ratio of permeability of water to that of organic solvents such as methanol or toxins.

Modeling of an amorphous polymer such as an sSIBS membrane is a considerable challenge due to the need to perform simulations at vastly different length and time scales. At the most fundamental level, we have to employ quantum mechanics followed by molecular dynamics (MD) to calculate the polymer density and diffusion properties. Modeling the morphology, permeability or mechanical properties of the microphase separated copolymer requires mesoscale level simulations. We use the dynamic density functional theory (DDFT) mesoscale approach followed by the finite element method utilizing the self-consistent homogenization theory to calculate macroscopic properties.

Here the mesoscale approach is described in greater detail with specific emphasis on a novel parameterization technique for block copolymers. A newly developed integration of the homogenization method with mesoscale simulations leading to accurate calculation of mechanical properties will be discussed.

The SIBS copolymer of interest in this work is comprised of approximately 30% PS, resulting in a morphology of hexagonally packed PS cylinders in a PIB matrix. Upon sulfonation of the polystyrene repeat units, solvent permeability increases dramatically (Elabd et al., 2003, 2004). At the percolation threshold of sulfonation, the distinct hydrophilic domains become interconnected and continuous, thus allowing water and ions to easily pass through the polymer. In the case of SIBS, it was found that the percolation threshold, which is characterized by a rapid increase in diffusion coefficients, is reached at about 20% sulfonation (Crawford et al., 2001). In addition, increases in sulfonation lead to increases in polymer density and particularly solubility.

In our recent work (Andzelm et al., 2006), an atomistic model for sSIBS copolymer was proposed and verified in calculations at various levels of sulfonation and water content. It was found that three water molecules are necessary to withdraw a proton from a sulfonic acid group. Both water and hydronium ions are linked through hydrogen bonds and reside near the sulfonated groups. Simulations clearly show a phase separation occuring between the ionic phase (SO_3^-, H_3O^+, H_2O) and the non-ionic region consisting of

Report Documentation Page

Form Approved
OMB No. 0704-0188

Public reporting burden for the collection of information is estimated to average 1 hour per response, including the time for reviewing instructions, searching existing data sources, gathering and maintaining the data needed, and completing and reviewing the collection of information. Send comments regarding this burden estimate or any other aspect of this collection of information, including suggestions for reducing this burden, to Washington Headquarters Services, Directorate for Information Operations and Reports, 1215 Jefferson Davis Highway, Suite 1204, Arlington VA 22202-4302. Respondents should be aware that notwithstanding any other provision of law, no person shall be subject to a penalty for failing to comply with a collection of information if it does not display a currently valid OMB control number.

1. REPORT DATE **01 NOV 2006**	2. REPORT TYPE **N/A**	3. DATES COVERED **-**
4. TITLE AND SUBTITLE **Multiscale Modeling of Polymer Membranes for Soldier Protective Clothing**		5a. CONTRACT NUMBER 5b. GRANT NUMBER 5c. PROGRAM ELEMENT NUMBER
6. AUTHOR(S)		5d. PROJECT NUMBER 5e. TASK NUMBER 5f. WORK UNIT NUMBER
7. PERFORMING ORGANIZATION NAME(S) AND ADDRESS(ES) **Weapons and materials Research Directorate, US Army Research Laboratory Aberdeen Proving Ground, MD 21005-5069**		8. PERFORMING ORGANIZATION REPORT NUMBER
9. SPONSORING/MONITORING AGENCY NAME(S) AND ADDRESS(ES)		10. SPONSOR/MONITOR'S ACRONYM(S) 11. SPONSOR/MONITOR'S REPORT NUMBER(S)
12. DISTRIBUTION/AVAILABILITY STATEMENT **Approved for public release, distribution unlimited**		
13. SUPPLEMENTARY NOTES **See also ADM002075., The original document contains color images.**		
14. ABSTRACT		
15. SUBJECT TERMS		

16. SECURITY CLASSIFICATION OF:			17. LIMITATION OF ABSTRACT	18. NUMBER OF PAGES	19a. NAME OF RESPONSIBLE PERSON
a. REPORT **unclassified**	b. ABSTRACT **unclassified**	c. THIS PAGE **unclassified**	**UU**	**33**	

Standard Form 298 (Rev. 8-98)
Prescribed by ANSI Std Z39-18

polyisobutylene and unsulfonated polystyrene groups indicated a lamellar-type structure of water molecules linked to the sulfonate groups. Studies of water self diffusion found a well-resolved jump distribution indicative of the hopping mechanism for self-diffusion with a jump length distribution quite different from that of pure water.

We have modeled two different sulfonated group distributions: blocky and dispersed. Based on calculated self-diffusion coefficients, we have found that the blocky architecture improved water diffusion. This can also be confirmed qualitatively by comparing the "surface accessible to water" (SAS) which in the blocky case appears to be continuous, while the SAS surface is broken for the dispersed architecture. This could be interpreted as the ability of the blocky architecture to open channels for water diffusion. We concluded that the blocky architecture achieves a percolation threshold at lower sulfonation level than that of the dispersed architecture. Therefore, it might be beneficial to synthesize polymer membranes with sulfonated groups precisely blocked within the localized polystyrene phase.

In the present paper, we applied the multiscale technique to improve our understanding of sSIBS properties particularly at higher sulfonation level. We will present results of quantum chemistry calculations on models of sulfonated styrene monomers surrounded by cluster of water molecules to elucidate the binding mechanism between water molecules, hydronium ion and sulfonated group of styrene. Next, the MD simulations will be presented for the range of sulfonation levels already published, 22% to 82%. Preliminary results for membrane structures in the presence of metal ions, such as Mg, Ca, Ba and Cs will be given. It is known that alkali metals decrease water permeability, but they also exhibit superior selectivity with respect to chemical agents as dimethylmehtylphosphonate (DMMP) (Crawford et al., personal communication). The molecular structure is largely unknown and of particular interest is the role of metal ions in cross-linking sulfonated groups. We will also propose a new atomistic model based on the lamellar morphology of a block copolymer and discuss permeability of water into sPS and PI phases of sSIBS. Finally, we will show our initial results from the mesoscale modeling of morphology for SIBS and sSIBS copolymers. The effect of blending with PS and PI and also containment within slab or nanopore field on morphology will also be explored.

2. METHOD

2.1 Multiscale Modeling

Theoretical studies of polymer membranes that are both accurate and predictive require use of multiscale modeling (Muller-Plathe, 2003). This requirement emerges naturally from the fact that the interactions of atoms at the level of Angstroms and femtoseconds determine macroscopic properties of a polymer at the macroscopic scale of micrometers and milliseconds and beyond. It is well known that atomistic details, stereochemistry, sequence of monomers and topology influence significantly macroscopically observed behavior of polymers. For example, sulfonation of SIBS triblock copolymer makes it permeable to water.

Multiscale modeling linking fundamental quantum and macroscopic, continuum theories of material, allows in principle for unbiased, ab inito and rational discovery of new materials and its properties. With the advent of high-speed parallel supercomputers and development of so called order N algorithms, it is tempting to assume that one day we will be able to perform calculations for billion atoms using fundamental ab initio quantum mechanical methods. We are, of course, very far from such possibility but even if ever realized it may not be

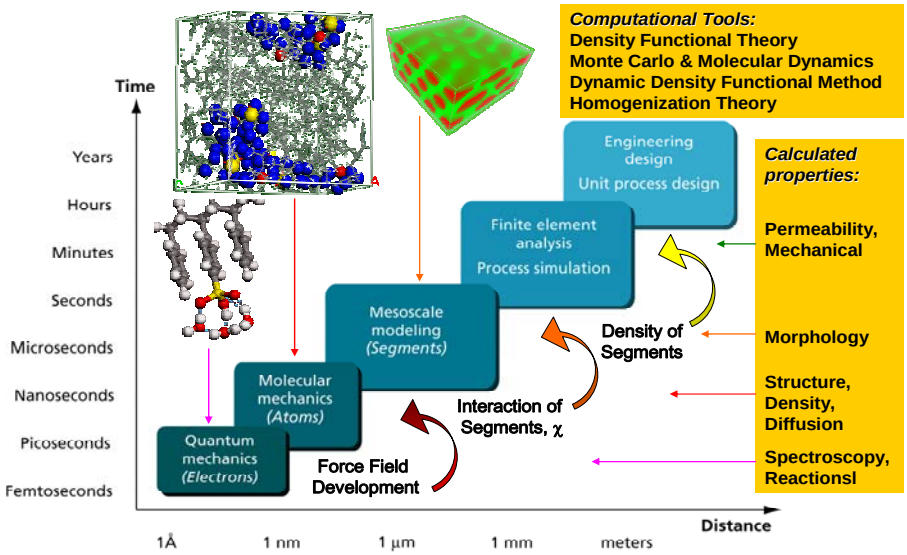

Figure 1. Multiscale modeling of amorphous polymers

useful as it would provide mountain of unnecessary detailed data on electron and atomic dynamics that is not needed if one asks a larger scale question about e.g. polymer coil size or morphology. The paradigm of multiscale modeling is appealing because it assumes use of data from lower level of calculations to parameterize computational models at the higher level, thus hiding unnecessary details of lower level theory and making simulations practical and focused on calculated properties easily accessible to experiment.

Still, multiscale simulations of polymer membranes are computationally very demanding because of the need to accommodate quite different length and particularly time scales. If we consider one of the simplest polymers, polyethylene, the distance between atoms of the polymer chain is about 0.1 nm and this chain can form a coil of 10-100 nm in diameter. Molecular vibrations occur at 10^{-13} s and bond rotations at 10^{-11} s while the chain relaxation time can be 10^{-4} s or much larger at lower temperatures near the glass transition temperature. Therefore, the multiscale approach requires use of various methods applicable to bridge the gap of at least 4 orders of magnitude in the length scale and 9 or more orders in the time scale (see Fig 1).

In this paper, we are concerned with four components of polymer multiscale simulations (Yip et al., 2005) (Fig. 1): (i) quantum mechanical solutions of Schrodinger equation providing electronic properties of molecules and possibility to study bond breaking and chemical reactions, (ii) molecular mechanics and dynamics considering only atoms movement by solving Newton- type equations, (iii) mesoscale modeling of polymer structure using segments (beads) obtained through coarse-graining polymer chain and (iv) finite element analysis by imposing a grid on a mesoscale and calculating permeability or mechanical macroscopic properties. We have primarily used Density Functional Theory (DFT) for our quantum mechanical calculations while Molecular Dynamics and Monte Carlo programs were used at the atomistic modeling step. Results of quantum calculations provided us with basic understanding of reactions between water molecules and sulfonated group of sSIBS (see Fig 1) and also allowed us to parameterize the interaction potential between atoms of the polymer, the so called Force Field necessary for the atomistic simulations of sSIBS. Molecular Dynamics simulations yield information about the atomistic structure, density of polymer and properties such as diffusion of water molecules through the polymer membrane.

In order to calculate morphological features of a polymer at the 20-1000 nm range, we had to create a coarse-grained model of a polymer by dividing the chain into segments (beads). The Molecular Mechanics step of multiscale simulations serves also as a source of parameters for the mesoscale modeling providing information about interactions between segments of a polymer. We have used Dynamic Density Functional mesoscale method as implemented in MesoDyn program (Fraaije et al., 1997). This approach allows representing polymer morphology through the density fields such as displayed in Fig.1 morphology of a SIBS slab with polystyrene phase (red) and polyisobutylene phase (green). The final step of our multiscale modeling involves application of the Homogenization Theory to calculate macroscopic mechanical properties by using density of segments from mesoscale generated structures as input. We have also used a Mesoprop program that solves Laplace's equations to calculate permeability of a system using mesoscale structures as an input.. Calculations involving quantum and atomistic simulations are computationally quite intensive and require use of MSRC supercomputers, while the visualization of calculated structures and properties was done at a desktop computer using Materials Studio software (Materials Studio, 2005).

2.2 Quantum and Atomistic modeling

Details of quantum and atomistic modeling for sSIBS copolymer were presented in our previous paper (Andzelm et al., 2006) and will be only briefly repeated here. Quantum mechanical calculations were performed using DFT as implemented in DMol program. Molecular structures and reaction path of proton dissociation from the sulfonated group were found using efficient optimization technique involving delocalized internal coordinates. Atomic charges were calculated from a fit to the electrostatic potential obtained from Dmol calculations. These charges were used to validate force field (COMPASS) used in the atomistic simulations.

The initial model of amorphous polymer including water molecules and ions was constructed with the Amorphous Cell program of Materials Studio. This is a Monte Carlo technique that calculates the initial structures of a polymer. Subsequently, the structures are energy minimized and subjected to several annealing steps to allow for proper distribution of small molecules and ions in the unit cell. Density determination was done using NPT ensemble, while water diffusion was studied with the NVE ensemble. The equations of motion were integrated using the Verlet algorithm with a time step of 1fs. To facilitate calculations, the nonbonded interactions were calculated using the charge group approach.

2.3 Mesoscale modeling

The morphology of SIBS copolymer at the mesoscale level was studied using the MesoDyn program (Fraaije et al., 1997, Materials Studio, 2005). MesoDyn

considers dynamics of density distribution of polymer beads, ρ_I in the field of external and mean-field interaction potential of density concentration.

The polymer chains are divided into beads that correspond to the Kuhn statistical segments and the polymer chain is modeled as so called ideal Gaussian chain. The modeling of interaction between beads involves use of the Flory-Huggins χ parameter. When system is away from equilibrium, the density distribution of polymer beads, ρ_I evolves according to the Langevian stochastic diffusion equations:

$$\delta\rho_I / \delta t = M \nabla\rho_I \nabla\mu_I + \eta$$

where μ_I is the intrinsic chemical potential that is derived from the differentiation of the free energy with respect to the density. Here M is a bead mobility parameter and η is a thermal noise. These equations are solved on a cubic mesh by a Crank-Nicholson scheme.

2.4 Parameterization of MesoDyn model

Details of parameterization will be given elsewhere and here we will briefly discuss generation of two key input parameters for this mesoscale model:

- polymer beads length
- Flory-Huggins interaction parameter between beads

We consider two phases of SIBS copolymer: polystyrene (PS) polyisobutylene (PI) and in the case of sSIBS polyisobutylene (PI) and the sulfonated polystyrene (sPS). Since our coarse-graining mesoscale model includes many monomers of styrene that are randomly sulfonated, it would be impractical to distinguish sulfonated and non-sulfonated phase of sSIBS. This can be done only at the monomer level and that was indeed done in our atomistic MD simulations but it would defeat the purpose of coarse-graining for the mesoscale model.

To estimate interactions between beads of PS, sPS and PI, we selected the Hildebrand formula to calculate the Flory-Huggins mixing χ parameter:

$$\chi = (\delta_I - \delta_J)^2 / RT\, V_{ref}$$

where V_{ref} is a reference volume of interacting beads and δ_I stands for the solubility parameter of phase I that can be obtained from $\delta_I = (E_{coh}/V)^{1/2}$. Accurate determination of cohesive energy density, E_{coh} requires an extensive exploration of configurational space at the MD level and therefore we have also used a semiempirical method, SYNTHIA that applies the topological information about polymer to calculate various physicochemical properties.

Since the Flory-Huggins model requires use of only one reference volume, we have to adopt a coarse-graining strategy that define beads based on a similar volume instead of strictly mapping the polymer to the equivalent Gaussian chain. Taking into account the MD calculated densities of PI and PS phases, we find that SIBS copolymer has about 28% PS volume that would correspond to the A3B15A3 architecture, where A represents a bead of PS and B a bead of PI. Using molar volumes of PS and PI monomers, we find that the mesoscale bead volume is approximately filled with 26 and 38 monomers of styrene and isobutylene, respectively. To calculate solubility parameter of PS(PI), we performed MD simulations using 3 oligomers each of 30(40) monomers of styrene(isobutylene). After 500ps NVT equilibration, the cohesive energy was calculated and using Hildebrand formula the interaction parameter χ was found to be 2.38.

In the case of sulfonated SSIBS copolymer, a similar coarse-graining strategy was used. The relative volume of sPS phase was calculated using density obtained from MD simulations (see section 3.2). Taking into account the increase in the mass of sPS phase because of the water present, leads to a 32%- 34% relative content of sPS phase and allows us to propose an architecture of S3B12S3 and S3B11S3 for membranes with 22% and 82% sulfonation, respectively.

The interaction between beads sPS(S) and PI(B) can not be easily calculated using the approach as presented above for SIBS. This is because the Flory-Huggins formalism is valid for weakly interacting systems and not for ionomers with water. The MD calculations of solubility parameter for water result in extremely high value of about 48 $MPa^{1/2}$, above any typical polymer. We have performed SYNTHIA calculations for the acidic form of sulfonated styrene monomer. Both Fedor's and van Krevelen values of solubility are close to each other with an average value of 24.7 $MPa^{1/2}$. To calculate the solubility parameters of sSIBS at various levels of sulfonation, the PS-PI interaction energy, χ of 2.38 was increased by the ratio of sulfonation, resulting in χ parameter of 4.28 for the 82% sulfonation.

We found that the morphology results are not sensitive to increasing interaction parameters by about 50%, however at larger values, the Crank-Nicholson scheme failed to converge. The influence of electrostatic field was also studied by using the Donnan approximation and no major changes to the morphology results were observed.

2.5 Finite Elements Analysis

Finite elements are necessary to quantitatively analyze the results of the mesoscale calculations. The most commonly used approach of solving Laplace's equations, as implemented in Mesoprop program provides only approximate results of mechanical

properties. Traditional Reuss and Voigt bounds are known to provide lower and upper bounds, respectively, through the theory of minimum potential energy. These are often too broad to provide a reasonable understanding of the material because typical volume or density fractions of solutions are in the range 40-60%, which is often the range in which the bounds are furthest apart.

We adopted the mathematical homogenization theory (Bennsoussan, et al., 1978) to estimate key *anisotropic* tensoral mechanical properties based on a knowledge of mesoscale morphology. The method relies on finite element solutions for the characteristic functions based on a mesh of the morphological features over a periodic unit cell and the density fractions at the mesh (or quadrature) points. Further details of implementation will be published elsewhere.

3. RESULTS

We will discuss results for polymer membrane as obtained at quantum mechanics, molecular dynamics and mesoscale level of multiscale calculations.

3.1 Quantum Mechanics

We have studied the deprotonation reaction of sulfonic acid using small models of sulfonated polystyrene oligomers surrounded by water molecules. Figure 2 presents DFT optimized structures of sulfonated styrene monomer with increasing number of water molecules. Individual clusters are stabilized by a network of hydrogen bonds. The hydronium ion (H_3O^+) is moved further from the sulfur atom from 3.286 Å to 4.090 Å with the increase of number of water molecules from 2 to 4, respectively. This effect was also noticed in our previous work by examining pair correlation functions from MD simulation.

A minimum of three water molecules surrounding sulfonic acid group are necessary to spontaneously withdraw the acidic proton. This was additionally confirmed by a computer experiment where one molecule and one hydronium ion were placed near the sulfonate group. In this case, the proton from the hydronium ion spontaneously was transferred to the SO_3^- group yielding acidic form SO_3H.

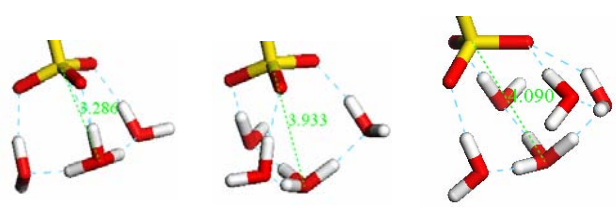

Figure 2. Structures of sulfonated styrene monomer with increasing number of water molecules. Hydrogen bonds are marked with broken line. Sulfur atom is yellow; oxygen is red and hydrogen is white.

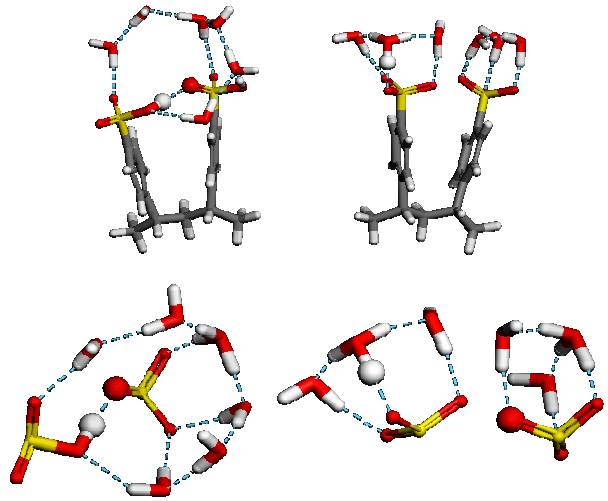

a) b)

Figure 3. Internal hydrogen bonding for blocky architecture of sSIBS copolymer.

The above conclusion is valid for dispersed sulfonated groups. In the case of blocky architecture, there is a possibility of a strong internal SO_3^- --H^+--SO_3^- hydrogen bonding protecting acidic proton from dissociation. Figure 3 presents a) conformation including internal hydrogen bonding and b) both acid protons are transferred to water molecules. The energy of breaking the internal hydrogen bonding is about 7 kcal/mol and the reaction path involves rotation of SO_3H group in the field of water molecules.

3.2 Molecular dynamics

The structure of sSIBS with metal ions was investigated at 64% sulfonation using the model from our previous work (Andzelm et al., 2006). Two water concentrations were studied corresponding to 5 and 10 water molecules per sulfonated group. The calculated self diffusion coefficients of water were similar to the experimental results and will be discussed elsewhere. Here we will discuss structural properties of membranes that can not be easily obtained from experimental measurements. Fig. 4a presents a unit cell of sSIBS model with 9 barium ions and 90 water molecules that can be considered as a model of a “dry” membrane. The continuous surface accessible to water (SAS) can be obtained by increasing the number of water molecules to e.g. 180 (see Figure 4b). Water molecules can diffuse within the lamella-type layers of SAS parallel to the plane of the unit cell. Examination of the 1.5ns NVE MD run leads to many structures with Ba ion surrounded by water molecules and also sulfonated groups. Some of these structures are presented in Fig. 4c. We have chosen a sum of van derWaals radii to find neighbors of Ba ion.

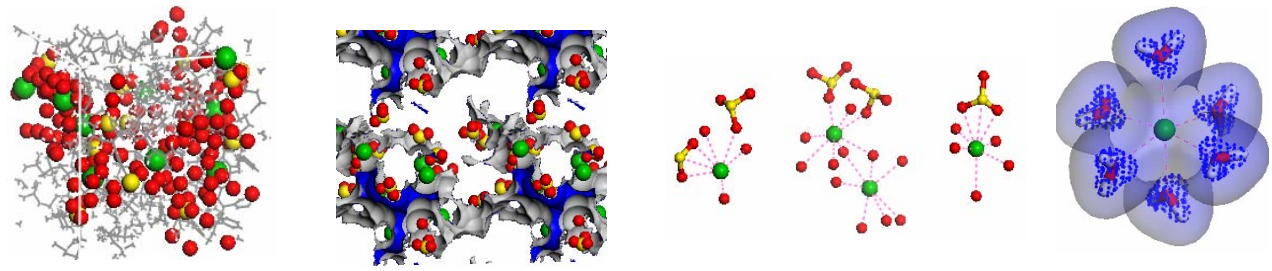

a) b) c) d)

Figure 4. sSIBS at 64% sulfonation with Ba ions. a) unit cell, b) surface accessible to water, c) selected clusters of Ba (green) interacting electrostatically with sulfonated groups (yellow) and water (single red ball), d) DFT density of $Ba(H_2O)_6^{+2}$ complex indicating deformation density of water molecules (blue dots).

Quantum mechanical (DFT) optimization of geometry leads to a complex of Ba^{+2} with 6 water molecules (Fig. 4d) and the Hirshfeld calculated charge of 0.8 a.u; a lower value than formal charge +2. Fig. 4d shows total density of this complex and also so called deformation density (total density -sum of atomic densities). One can see that deformation density (represented as dots) is only shown on water molecules indicating the ionic character of bonding in this complex. The bond energy is about 34 kcal/mol much higher that a typical hydrogen bonding of about 5 kcal/mol.

In summary, we found numerous structures indicating a cross linking between metal atoms and sulfonated groups with the participation of water molecules. Similar structures were found for sSIBS with Mg, Ca and Cs ions. We have calculated a radial distribution function of ions with sulfur and water to understand the relative distribution of ions and thus explain the decreasing water permeability in the presence of these ions. Integrating radial distribution functions at a distance up to ~4Å (end of the first shell) from the ion yields the following number of water molecules: 5.1, 5.5, 6.3 and 4.0 for Mg, Ca, Ba and Cs, respectively. These numbers when compared with the 3.2 obtained for the hydronium ion (no metals) indicate an increase in the number of water molecules localized in the shell around the metal ions. This is the primary reason for decreasing water permeability in the presence of ions.

We also found the following number of sulfonated groups in the neighborhood of metal ion within a first shell of~5 Å: 0.7, 1.5, 1.2, 0.8, 0.9 for hydronium, Mg, Ca, Ba and Cs ions, respectively. These results indicate that metal atoms are located closer to sulfonated group largely because of cross linking.

We will now describe a new MD model useful to study processes inside lamellar-phase of sSIBS. It is known that sSIBS forms a lamellar structure composed of two phases: sulfonated polystyrene and polyisobutylene. The spacing of these phases is more than 20 nm and therefore can not be entirely taken into account by MD simulations. A typical size of a unit cell in MD simulations can be about ~5 nm. Such a unit cell can include about 10,000 atoms and it is already computationally challenging if a sophisticated force field as COMPASS is used. One needs approximately one million atoms of polystyrene chains to fill a space of a unit cell with dimension of about 20 nm.

We performed MD simulations on small unit cells for two phases of sSIBS which results in a layered structure as presented in Figure 5. The entire slab has a length of about 9nm; 5nm of polyisobutylene and about 3nm of sulfonated polystyrene. Both phases were separately NVT equilibrated with amorphous unit cells built at previously NPT-optimized density. A thin layer of 80 water molecules was inserted between two material slabs. The the cell was allowed to relax under NVT (T=300K) thermostat and the density of water molecules was monitored along the slab distance, z. Water molecules enter only the polystyrene phase and within the next 6ns most of water molecules is already within the sulfonated polystyrene phase. This computer

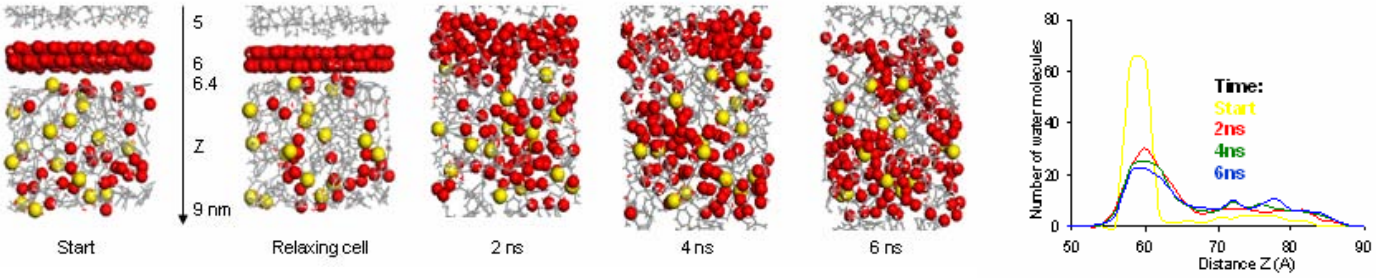

Figure 5. MD simulation of water (red) diffusion in the layer of polyisobutylene and sulfonated (yellow) polystyrene as a function of time. Plot indicates distribution of water molecules along the slab length (z) as a function of time in ns.

experiment provides additional justification for studying water diffusion only in the sulfonated polystyrene phase.

We have built amorphous cells of sulfonated polystyrene chains at various levels of sulfonation. The sulfonated groups were evenly spaced within the oligomer containing 36 styrene monomers and three oligomers were used in every unit cell. Using information from quantum mechanics calculations, we added 2 water molecules and one hydronium ion for every SO_3^- group in oligomers. The optimized density is presented in Table 1.

Table 1. Density of SPS phase, sSIBS copolymer as a function of sulfonation level, SL (in g/cm^3). The experimental values, Exp are included.

SL	SPS	sSIBS	Exp
17	1.18	0.99	0.97
22	1.25	1.00	0.99
29	1.32	1.02	1.03
42	1.48	1.06	1.09
64	1.73	1.14	
82	1.85	1.19	1.24

As expected, density of sulfonated polystyrene phase increases with sulfonation. Next we calculated a density of the entire sSIBS copolymer by including polyisobutylene phase with previously optimized density 0.892 and the .3084 weight fraction of polystyrene was used. Table 1 compares calculated density of sSIBS with the experimental values. The agreement within 3% is excellent and it also justifies the lamellar-type model of sSIBS. There are no experimental data of density available for sPS phase. Our previous model (Andzelm et al., 2006) that includes the entire copolymer is more appropriate to describe the border region of two phases sPS and IB.

3.3 Mesoscale simulations

Following the procedure described in section 2.4, we first performed Mesodyn calculations for the bulk and slab of SIBS using 32x32x32 and 32x32x19 grid, respectively. Fig. 6a shows hexagonal morphology of SIBS bulk that justifies our choice of SIBS Mesodyn architecture A3B15A3 and the Mesodyn interaction

Figure 6.Mesoscale structures of bulk SIBS (PS phase is red, PI phase is green). The right site does not show PI phase for clarity.

parameter, ε of 5.9. The calculations were started with a homogeneous melt and the phase separation process began almost immediately. The final morphology converged at ~8000 steps and does not depend on the grid size, however the phase separation does not occur for ε < ~4.5. We have modeled the slab confinement effects by introducing an effective interface-polymer interaction parameter $\varepsilon_M = \varepsilon_{AM} - \varepsilon_{BM}$. For negative values of ε_M, we calculate a wetting layer –type morphology with PS phase exposed to the surface of a slab and perforated lamella-type layers of PS phase at $\varepsilon_M = 0$ (Fig. 7a) turning into cylinders parallel to the surface for $\varepsilon_M = -5$. The positive values of ε_M result in number of morphologies such as PS cylinders perpendicular to the surface ($\varepsilon_M = 3$, Fig. 7b), parallel cylinders ($\varepsilon_M = 5$, Fig. 7c), and perforated-lamella for higher values of $\varepsilon_M > 10$ (Fig. 7d). For the positive values of ε_M, the PI phase is exposed to the slab surface.

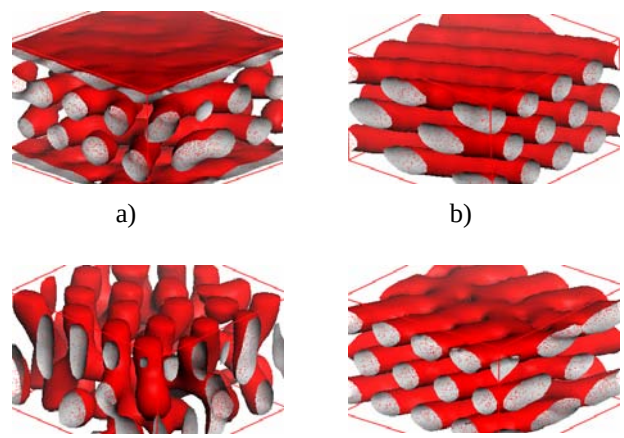

a) b) c) d)

Figure 7. SIBS thin-slab reconstructions as function of the strength of the surface field.

We have attempted to correlate the values of the ε_M parameter with the relative solubility parameters of solvents and PS and PI phases of SIBS. Considering that both cyclohexanone and PS have similar solubility parameters of 20.3 and 19.8, respectively, that should lead to a wetting layer morphology with a PS phase facing the surface of a slab we have identified as the structure in Fig. 7a (with $\varepsilon_M = 0$) as representative for this solvent. Consequently a solvent with a negative ε_M, such as cyclohexanol with solubility parameter of 23.3 should form a similar surface morphology, while solvents as chloroform or tetrahydrofuran may transform surface into parallel cylinders (Fig 7c) or lamellar phase (Fig 7d).

We have calculated the effect of sulfonation by changing architecture of copolymer to S3B12S3 and S3B11S3 and increasing Mesodyn interaction parameter to 7.3, 10.7 for 22% and 82% sulfonation, respectively (see section 2.4). As expected, calculations yield a

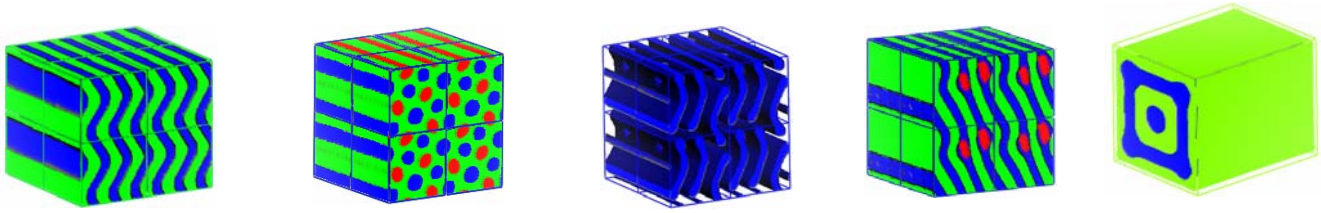

a) b) c) d) e)

Figure 8. Example of mesoscale morphologies of a) sSIBS, b) asymmetric PS-IB-sPS, c) blend with IB, d) blend with PS, e) sPS cylinder parallel to the walls of nanopore.

lamellar-type structure. Fig. 8a presents this morphology obtained using 24x24x24 grid. We have also studied morphology of asymmetric copolymer A3B15S4, corresponding to a copolymer with only one block sulfonated. Such architecture is similar to a blocky architecture and was found in MD simulations to increase water self diffusion. The asymmetric copolymer exhibits a cylindrical architecture (Figure 8b). The cylinders are composed of separated PS and sPS phases or mixed PS/sPS phase depending on the repulsion parameter between these two phases.

We have investigated morphology of sSIBS blends with polyisobutylene and polystyrene. Blends with polyisobutylene produced broken perforated lamella (Fig.8c), while blends with PS produced rods of PS inserted into the polystyrene phase of the sSIBS lamellar structure (Fig 8d). Finally, we have used newly developed code, based on the homogenization theory, to calculate mechanical properties of blends. As expected, increasing PS content increases Young's modulus, while blending with polyisobutylene decreases Young's modulus. We have also studied change in sSIBS morphology due to surface or nanopore confinement. Numerous structures have been identified, ranging from wetting layer through perforated lamella to lamellar as a function of the strength of the surface field. sSIBS in small nanopores forms cylinders parallel to the wall of the nanopore (e.g. Fig. 8e), which correlates with observed superior water permeability. Detailed discussion of mesoscale results will be presented elsewhere.

CONCLUSIONS

We have used multiscale modeling to understand atomistic and mesoscale structures of membranes that have potential to be useful for soldiers's protective clothing. Detailed structural information obtained in this work is not readily available from experimental measurements and may impact design of new membranes. In particular, molecular simulations led to prediction of a new blocky, non-symmetric architecture of polymer membrane that exhibits superior water permeability.

We have also presented development of integrated multiscale modeling system that is currently being used to study various materials of importance for warfighter such as batteries, polymer coatings, nano-composites and energetic materials.

ACKNOWLEDGEMENT

Authors would like to acknowledge helpful discussions with Dr. Betsy Rice. This work was partially done thanks to support of the Directors Research Initiative grant FY06-WMR-23. Computational resources of ARL and ASC MSRC are gratefully acknowledged.

REFERENCES

Andzelm, J.; Sloan, J.; Napadensky, E.; McKnight, S. and Rigby, D., 2006: Molecular Modeling Study of Sulfonated SIBS Triblock Copolymers, *Molecular Simulations*, **32**, 163-172.

Bensoussan A.; Lions J. L.; Panicolaou G.; 1978 *Asymptotic Analysis for Periodic Structures*, North Holland, Amsterdam.

Crawford D.M.; Napadensky E.; Tan N.C.B.; Reuschle D.A.; Mountz D.A.; Mauritz K.A.; Laverdure K.S.; Gido S.P.; Liu W. and Hsiao B., 2001: Structure/property relationships in polystyrene-polyiosbutylene-polystyrene block copolymers, *Thermochemica Acta*, **367**,125-134.

Elabd Y.A.; Napadensky E.; Sloan J.M.; Crawford D.M. and Walker C.W., 2003: Triblock copolymer ionomer membranes Part I. Methanol and proton transport, *J.Membr Sci*., **217**,227-242.

Elabd Y.A.; Walker C.W. and Beyer F.L.,2004: Triblock copolymer ionomer membranes Part II. Structure characterization and its effects on transport properties and direct methanol fuel cell performance, *J.Membr Sci*. **231**,181-188.

Fraaije, J. G. E. M.; van Vlimmeren, B. A. C.; Maurits, N. M.; Postma, M.; Evers, O. A.; Hoffman, C.; Altevogt, P.; Goldbeck-Wood, G., 1997: The dynamic mean-field density functional method and its application to the mesoscopic dynamics of quenched block copolymer melts, *J. Chem. Phys.*, **106**, 4260-4280.

Materials Studio 4.0, 2005: (Discover, Amorphous Cell, COMPASS, DMol, MesoDyn, SYNTHIA, Mesoprop), Accelrys.

Muller-Plathe, F., 2003: Scale-Hopping in Computer Simulations of Polymers, *Soft Materials*, **1**,1-31.

Multiscale Modeling of Polymer Membranes for Soldier Protective Clothing

25th U. S. ARMY Science Conference
November 30, 2006

Jan Andzelm, James Sloan, Eugene Napadensky, Rick Beyer, James Snyder, Peter W. Chung* and Steven McKnight

Army Research Laboratory,
Weapons and Materials Research Directorate,
Multifunctional Materials Branch
*AMSRD-CI-HC
Aberdeen Proving Ground, MD 21005

Acknowledgment: Mark VanLandingham, Betsy Rice, Brad Forch,
WMRD, DRI: FY06-WMR-23

Some parts of this work were published: Proceedings ACS, AIChE, 2005, 2006; Molecular Simulations, 32(2006) 163-172

Motivation

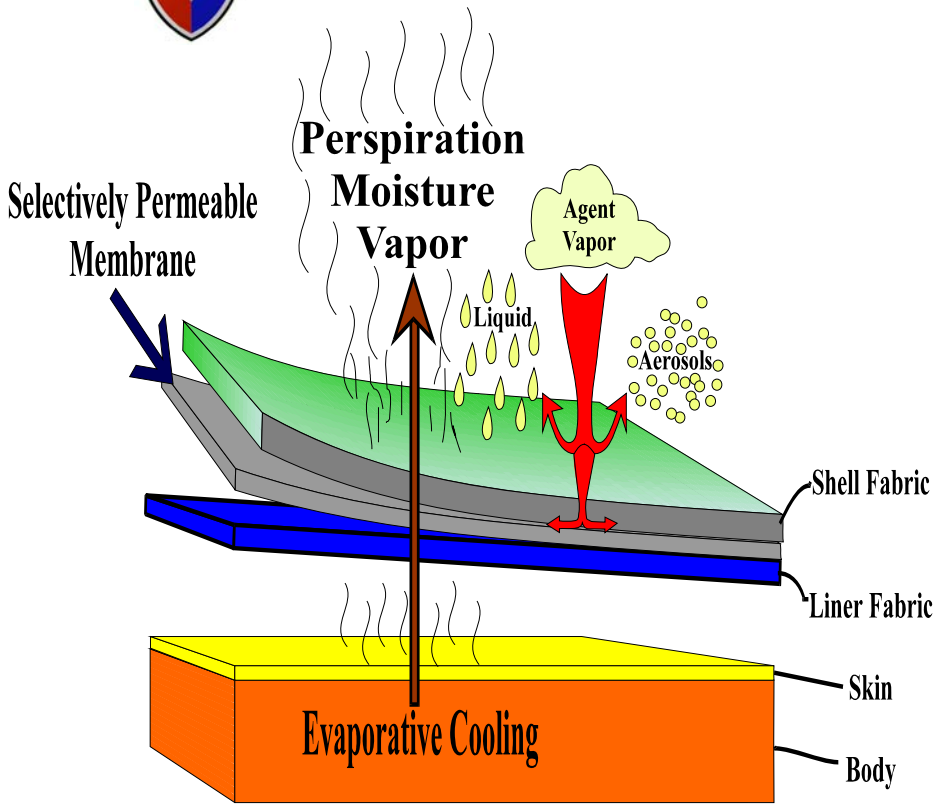

To understand and predict better polymer membrane materials that improve individual warfighter protection and sustainability

- **Reduced Weight**
- **Affordable**
- **Breathable and Protective**

<u>High water</u> permeability

Low warfare agents

Outline

1. Permselective barriers for soldier protection

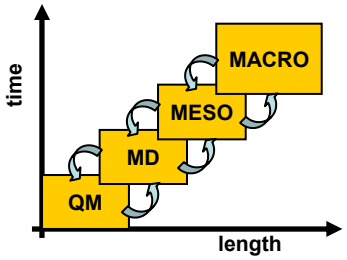

2. Multiscale modeling in polymer research

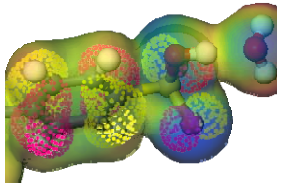

3. Understand bonding of water and membrane

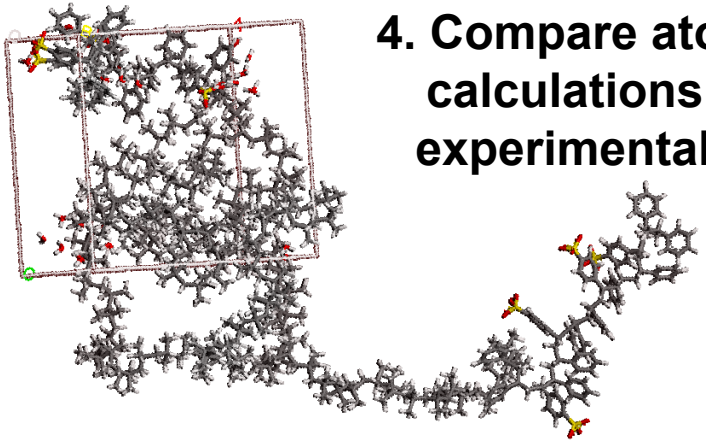

4. Compare atomistic calculations with experimental data

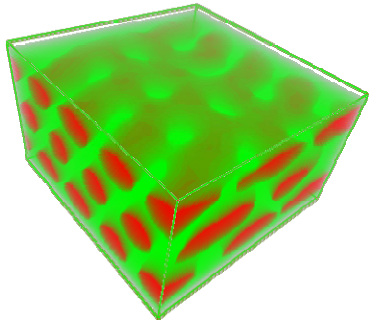

5. Predict new architecture and morphology of polymer membrane

Block-Copolymer as a Permeable Membrane for Soldier Protective Clothing

Block Copolymer: sulfonated polystyrene-polyisobutylene-polystyrene (S-SIBS) is a good candidate for a permeable membrane

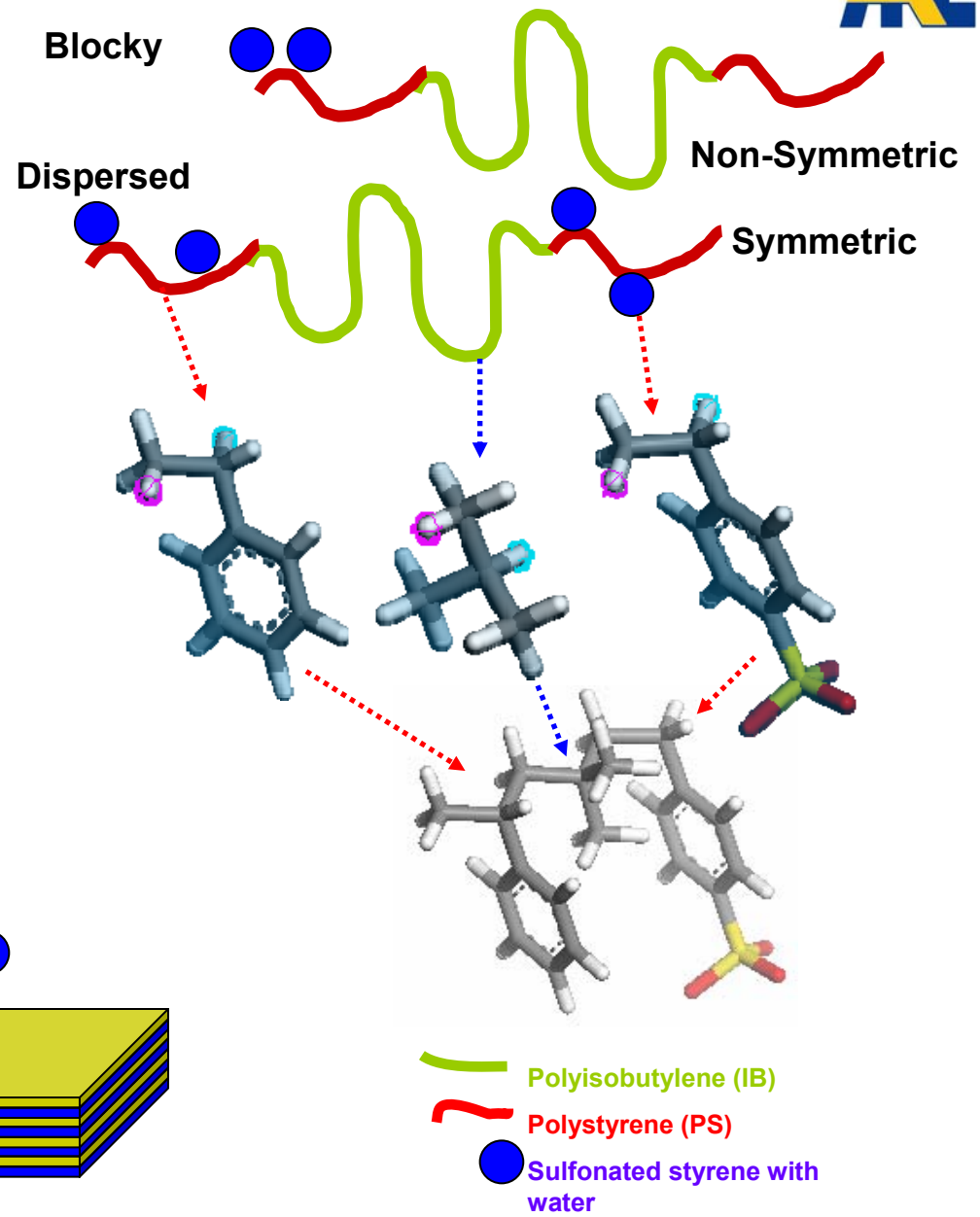

Block Copolymer Morphology

Cylinders

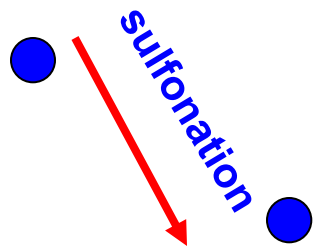

Ionomer Morphology

Lamellae

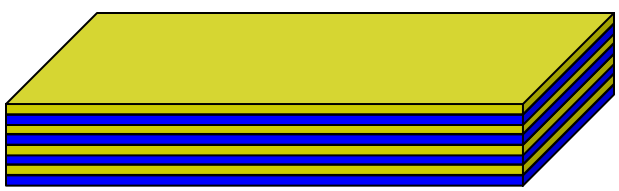

Need for multiscale modeling

Billion atom calculations from first (quantum) principles??
- neither feasible computationally nor scientifically desirable

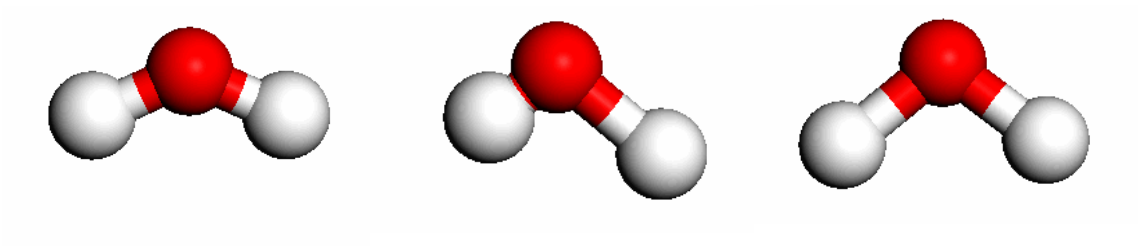

Vibration modes of water molecule

Polymer length scales :
- **Bond length ~ 1Å**
- **Micelle ~ 100 Å**
- **Lamella ~ 500 Å**

Polymer time scales :
- **Molecular vibrations 10^{-13} s**
- **Chain relaxation $>10^{-5}$ s**
- **Phase separation $>10^{-3}$ s**

Hexagonal morphology

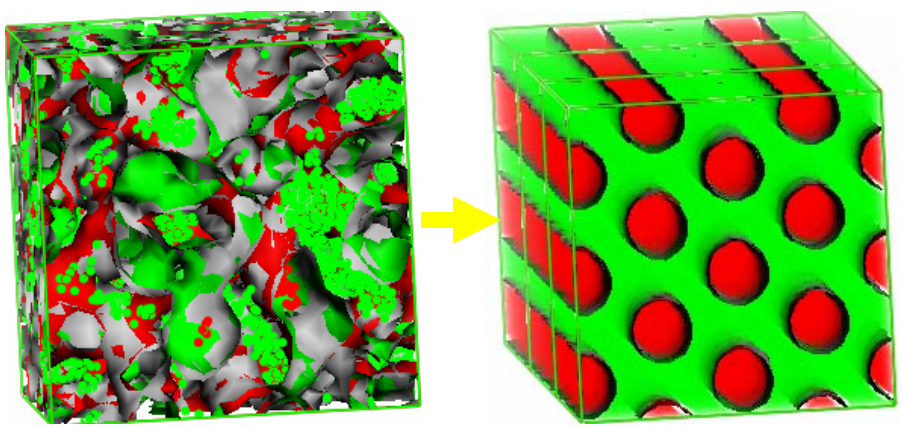

Formation of micelles

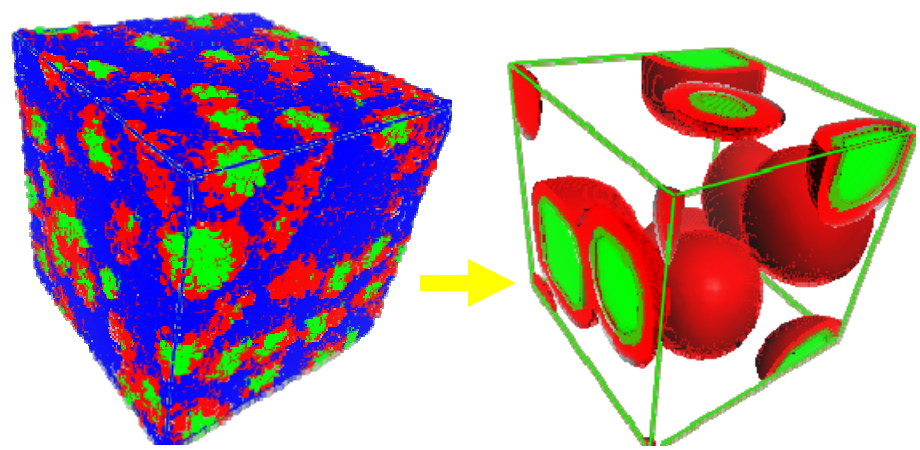

Multiscale Modeling of Amorphous Polymers

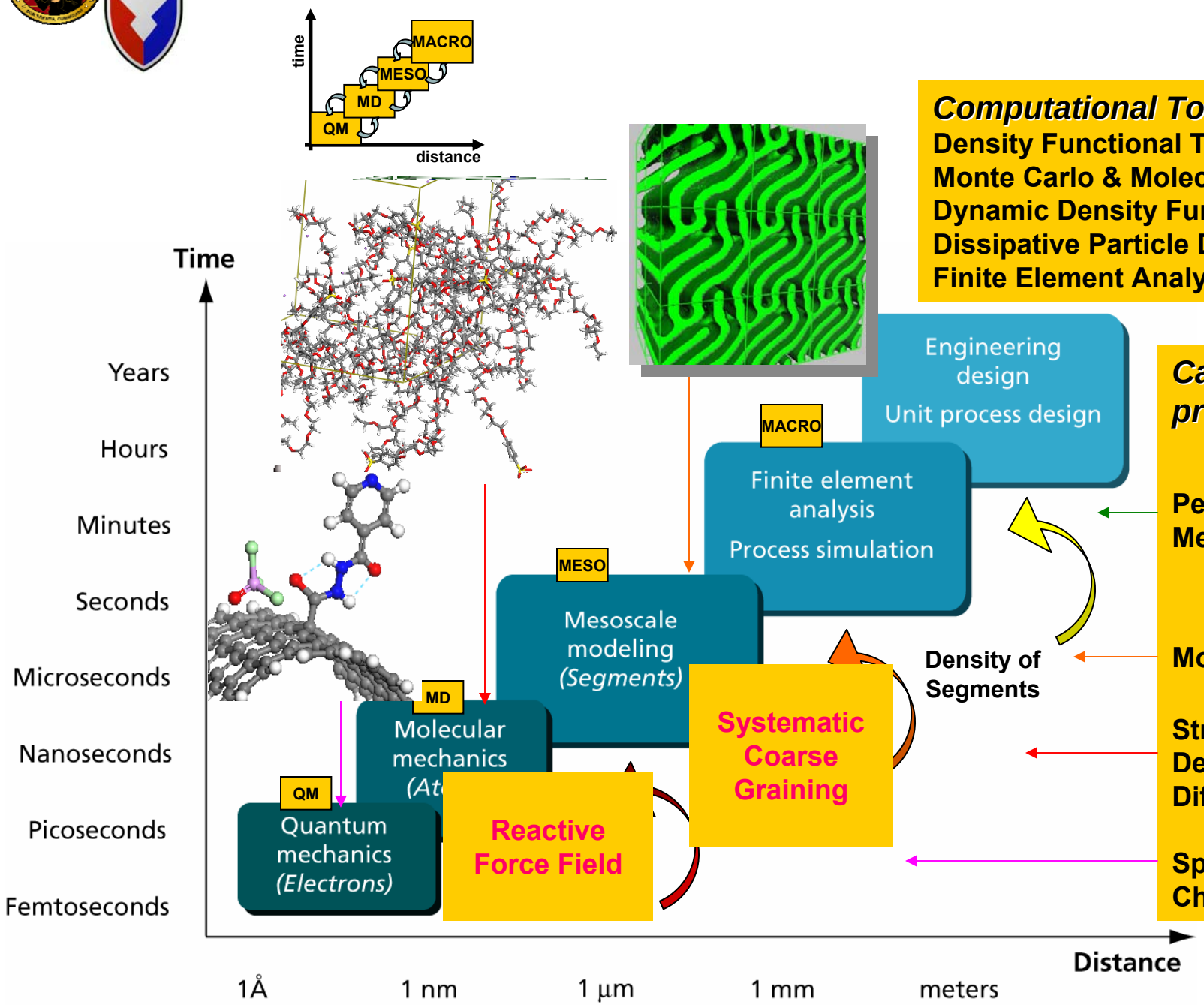

Computational Tools:

Density Functional Theory
Monte Carlo & Molecular Dynamics
Dynamic Density Functional Method
Dissipative Particle Dynamics
Finite Element Analysis

Calculated properties:

Permeability, Mechanical

Morphology

Structure, Density, Diffusion

Spectroscopy, Chemical reactions

Chemical reactions of water and sulfonate groups

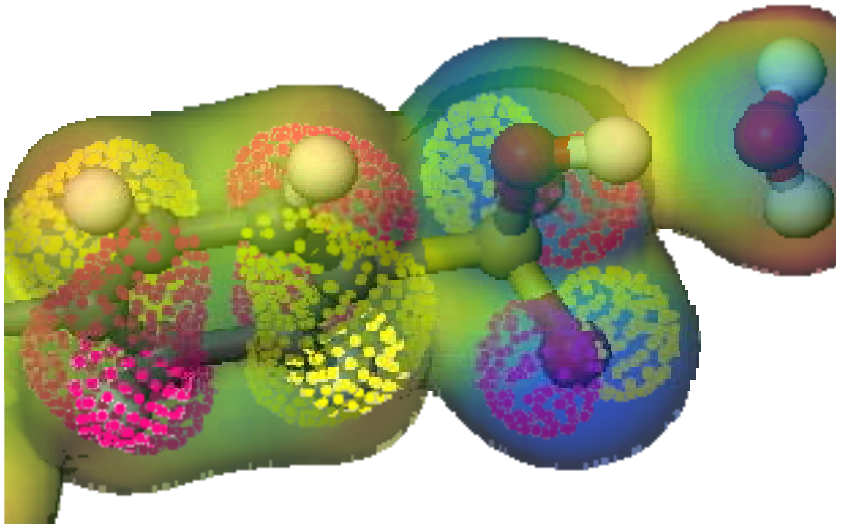

Electrostatic interaction in SO_3H- H_2O complex:
HOMO orbital (dots) & total density with mapped electrostatic potential

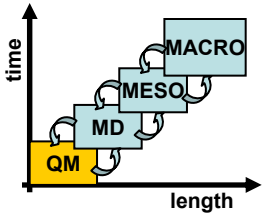

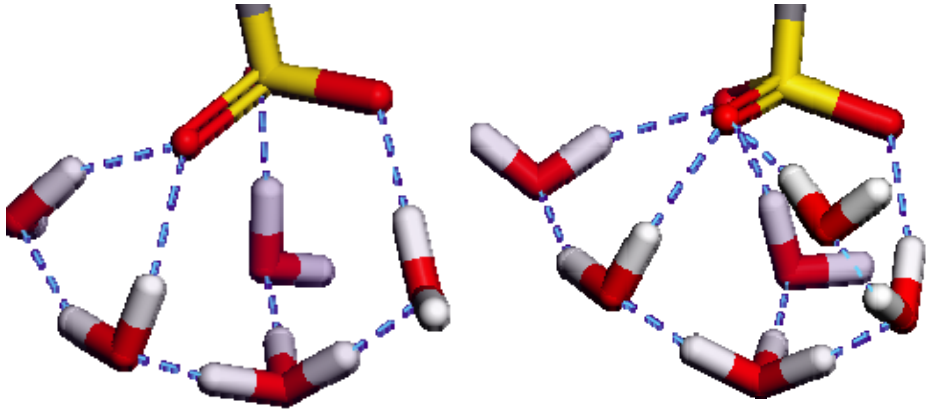

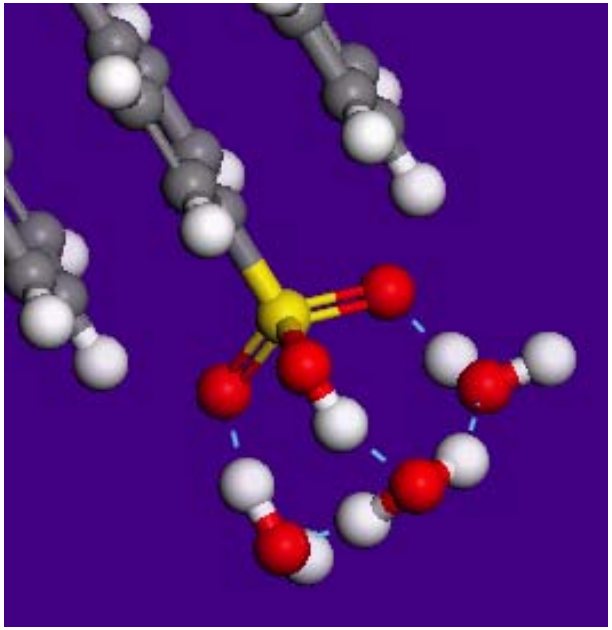

Spontaneous dissociation of proton (from SO_3H) occurs in the presence of minimum three water molecules.

Sulfonate group and water molecules are connected via ionic bonds

Dry S-SIBS may contain 3 waters/sulfonate group(SO_3^-)

Analysis of Molecular Dynamics calculations:

Distribution of water and hydronium ions in S-29-SIBS (29% sulfonation)

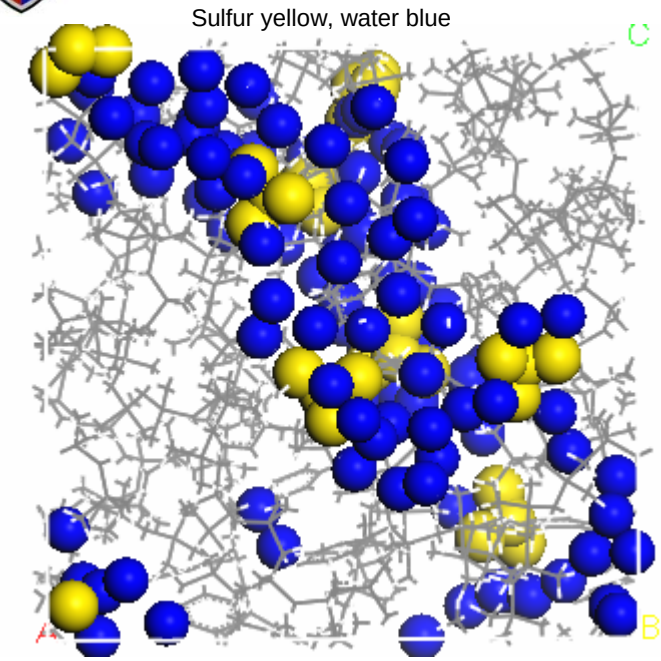

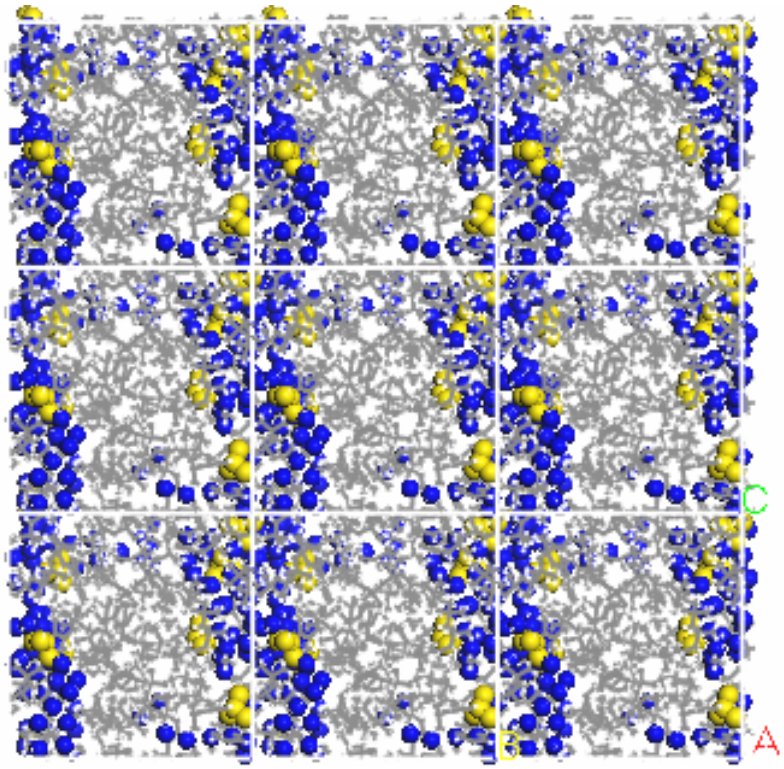

Water forms lamellar-type phase of connected pathways of H-bonded water-hydronium-sulfonate group

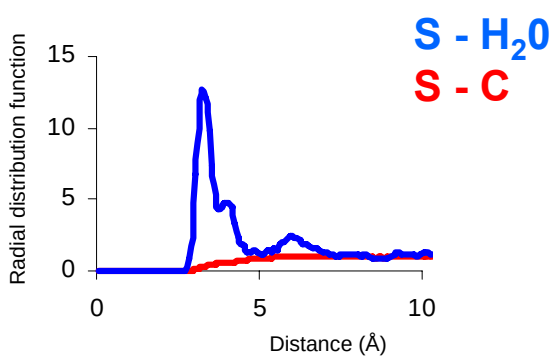

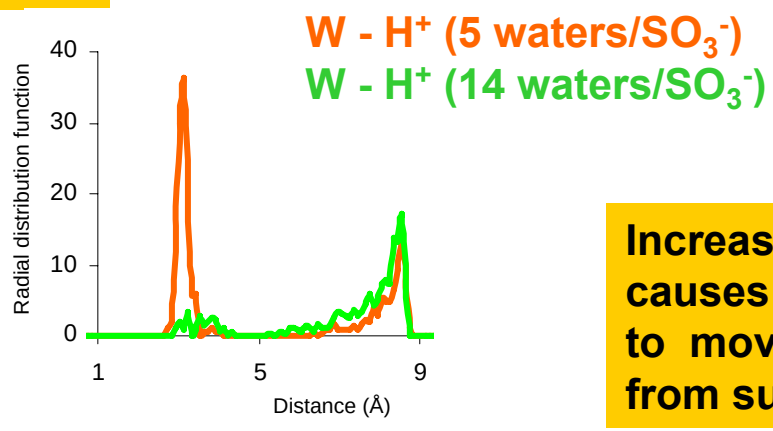

Increase of water content causes hydronium ions H^+ to move further away from sulfonate groups

Mechanism of water diffusion

Sulfur yellow, oxygen red, hydrogen white

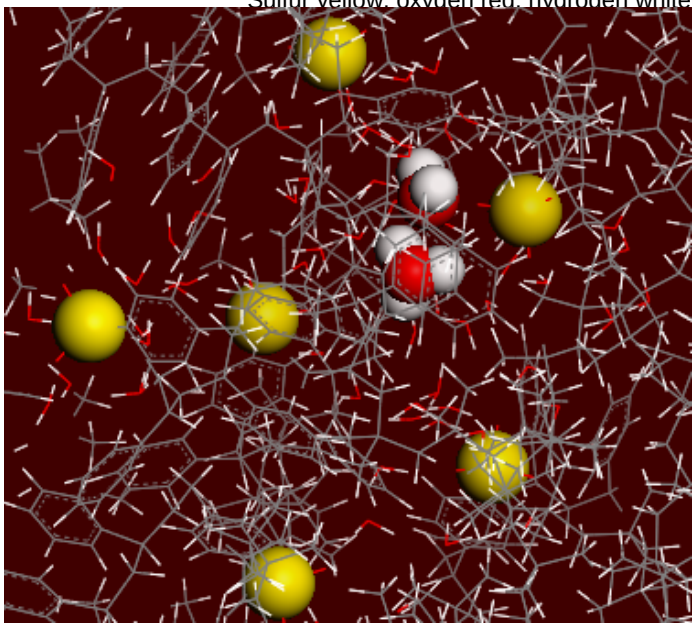

Atomistic model of polymer

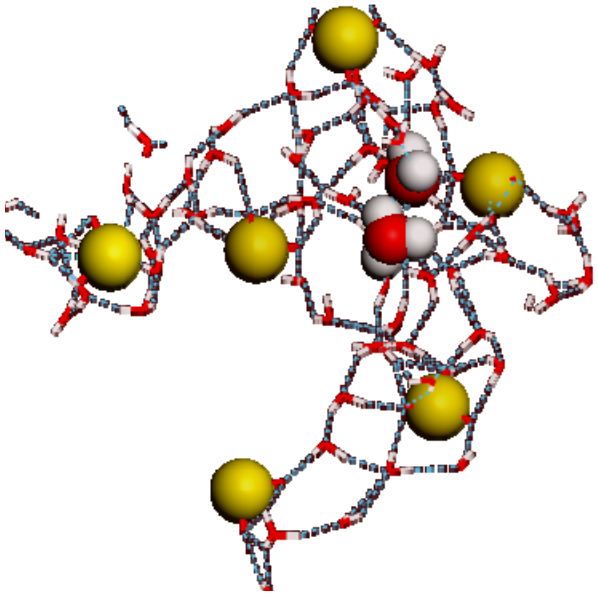

Network of hydrogen bonds

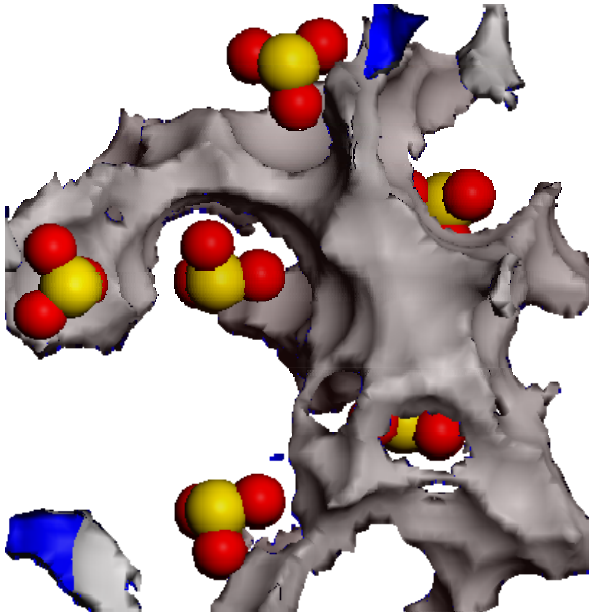

Surface accessible to water

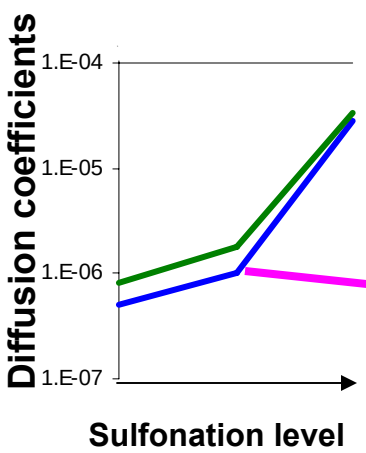

Calculated diffusion coefficients (and polymer density) follow closely **Experimental** data

Water diffusion increases dramatically at the percolation threshold of ~20% sulfonation

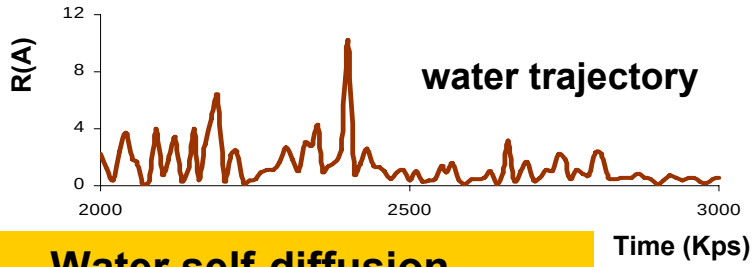

Water self-diffusion can be explained as hopping of water molecules between temporary voids in the polymer

Self diffusion of water D(x10^{-6} cm^{2}s^{-1})

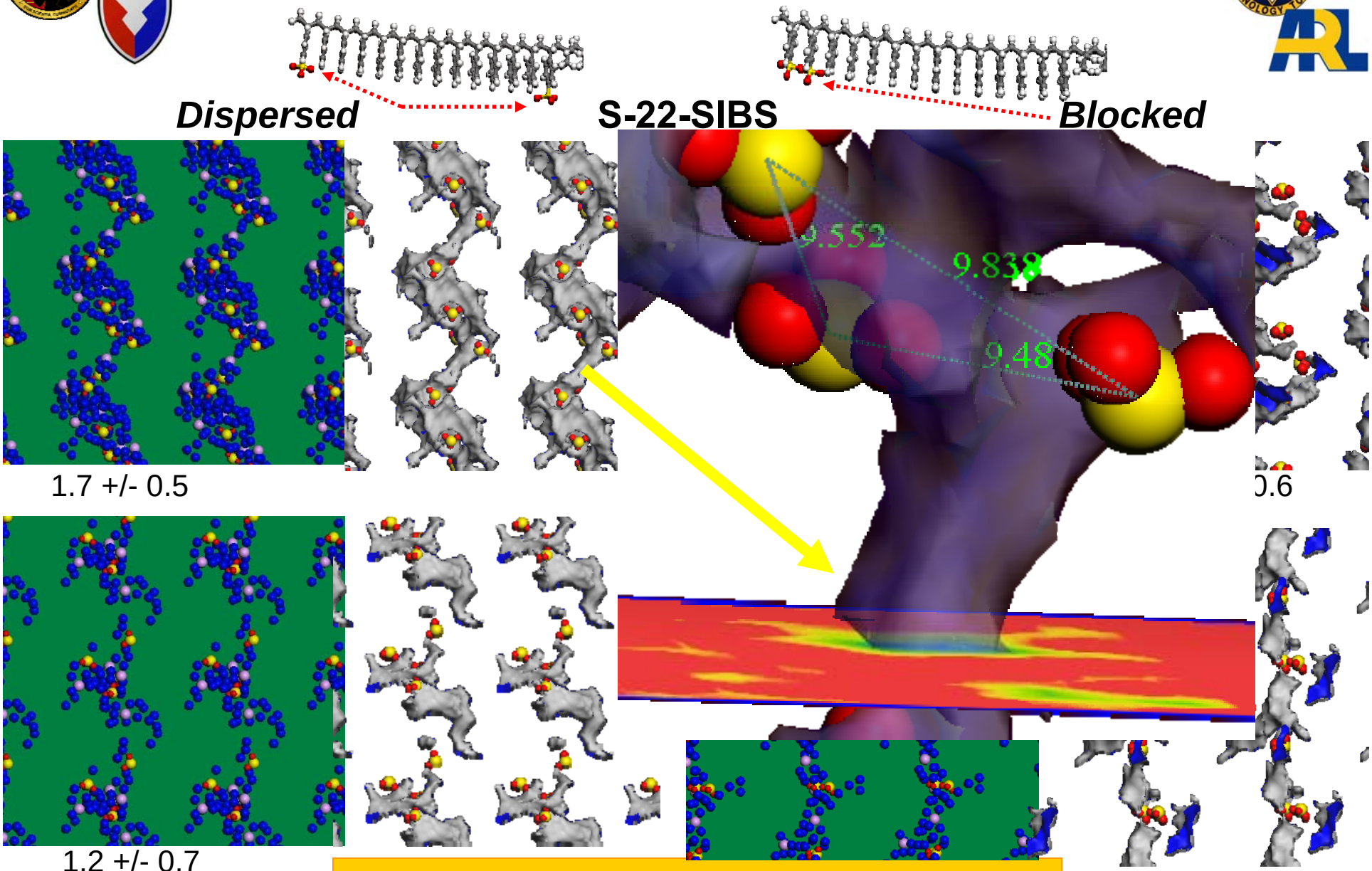

Water blue; sulfur yellow; oxygen red;
water accessible surface with probe 1.4A

***Blocky* architecture increases diffusion of water and lowers percolation threshold**

Interaction of Water, Sarin, Mustard gas with Dispersed and Blocky slab of S-22-SIBS

Selectivity = interaction energy of water / interaction energy of agent

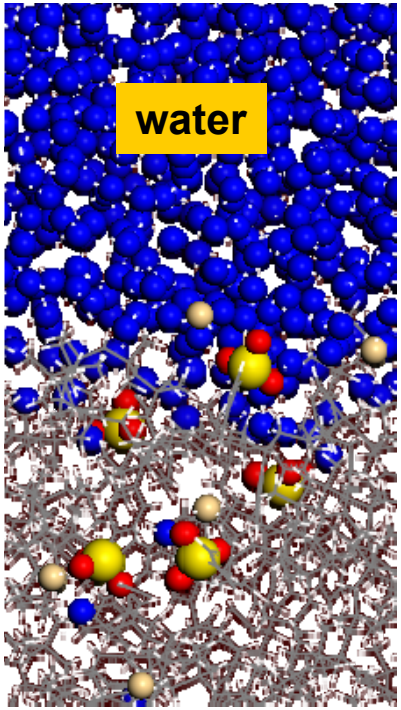

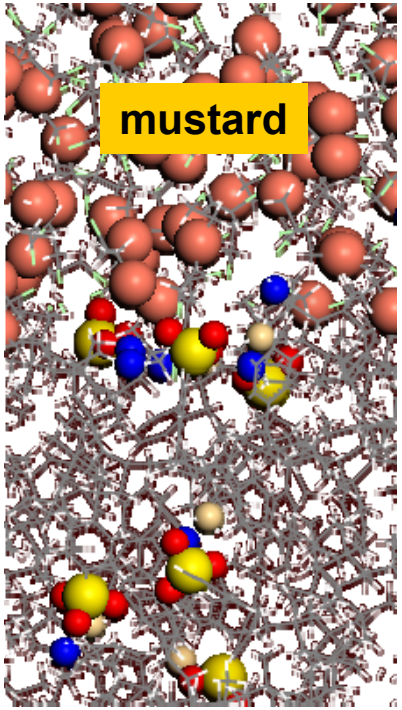

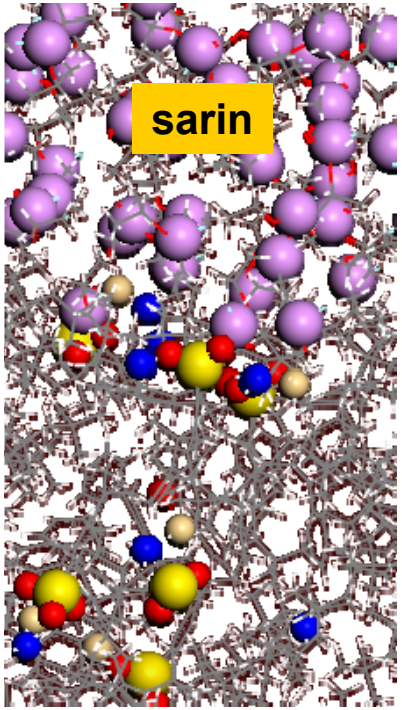

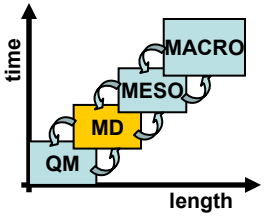

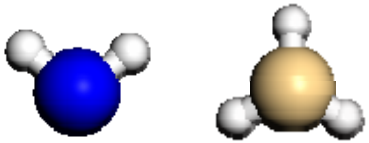

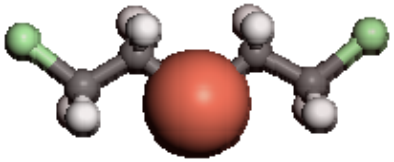

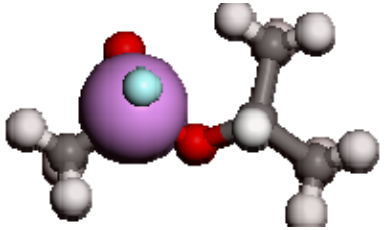

SO_3^- on a surface/	*Dispersed*	*Blocky*
High		
mustard	3.2	4.8
sarin	3.3	4.6
Low		
mustard	0.45	0.5
sarin	0.5	0.6

Presence of SO_3^- on a surface improves water binding and selectivity
Mustard gas & Sarin form stronger than water bonds with surface of polyisobutylene
***Blocky* architecture enhances selectivity**

Morphology of SIBS

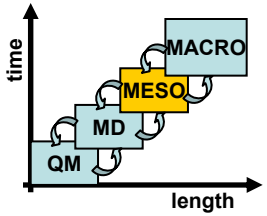

- Polymer divided into beads: S (polystyrene), IB (polyisobutylene) and S-S(sulfonated polystyrene with a small (5% or 10%) content of water)
- Flory-Huggins interaction parameter χ is used to model interaction between beads
- Relative solubility of S ,IB and S-S calculated using Molecular Dynamics

Hexagonal

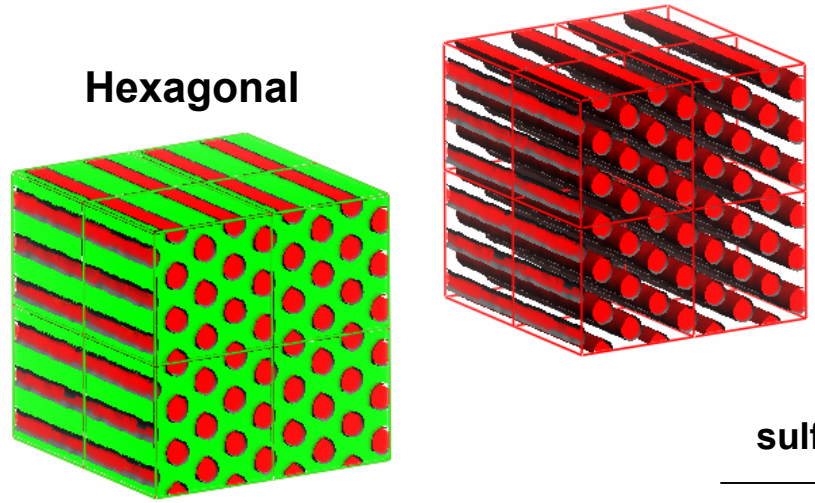

sulfonation →

Lamella

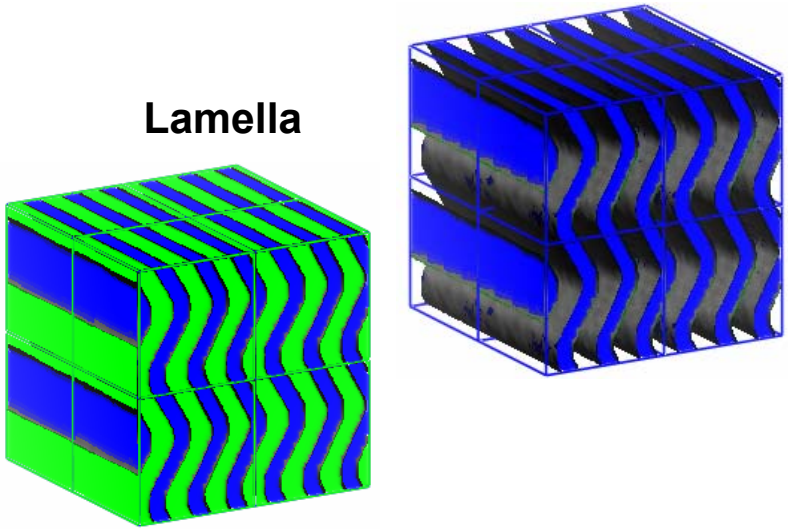

Hexagonal

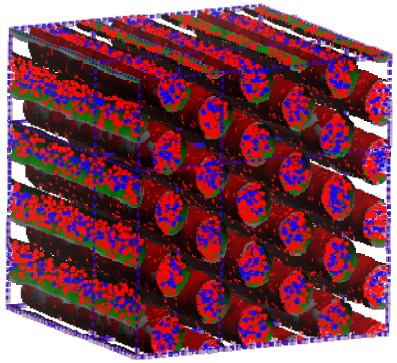

Modeling predicts that blocky and non-symmetric architecture increase diffusion of water and lower percolation threshold

Hexagonal morphology of non-symmetric S-SIBS

Polystyrene, Polyisobytylene, Sulfonated polystyrene with water

Phase Diagram of PS-PI

(A-B)(A=red)

Experiment: Eskimergen et al. Macromolecules 38(2005)1286.
Modeling: Mesoscale Modeling with Mesodyn

A9B3(f=0.25) high repulsion

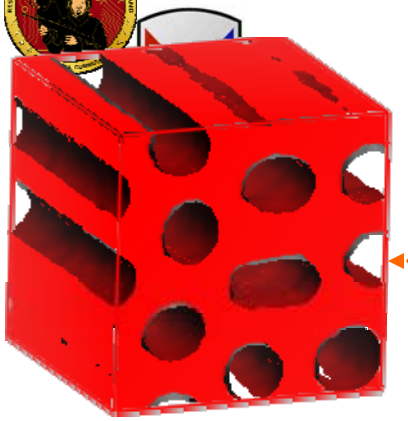

A9B3(f=0.25) low repulsion

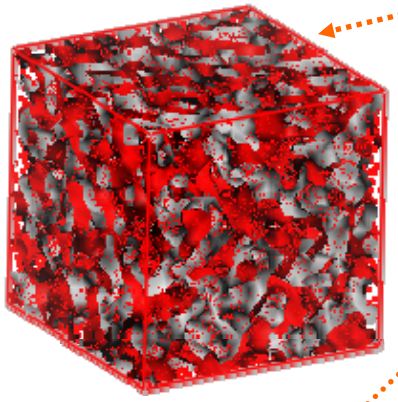

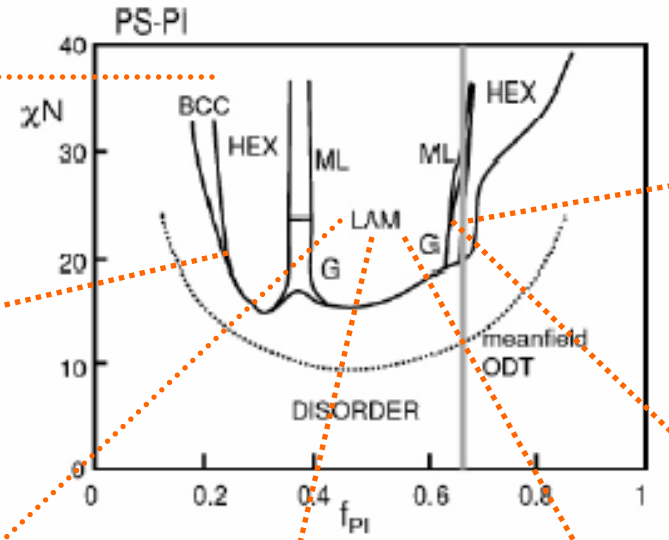

Figure 1. Phases of PS−PI diblock copolymers.[24] The $f = 0.67$ sample used for the present study is highlighted by the solid gray line.

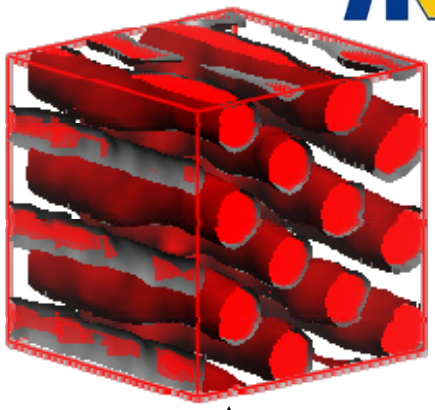

A4B8(f=0.67)

shear

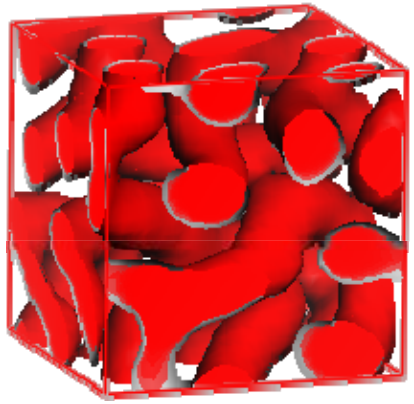

A7B5(f=0.42)

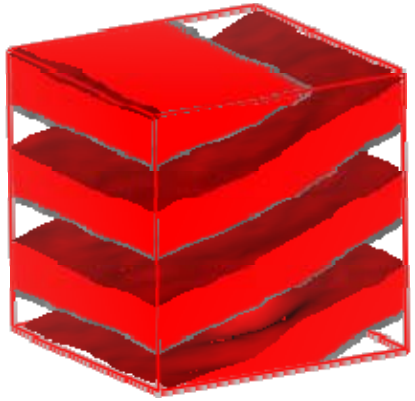

A6B6(f=0.50)

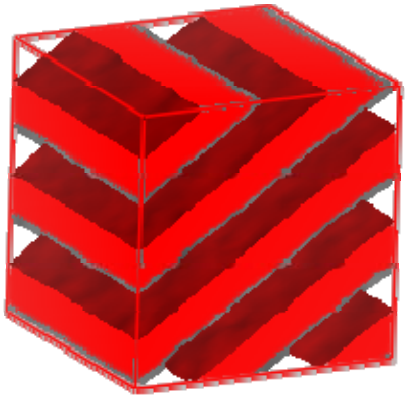

A5B7(f=0.58)

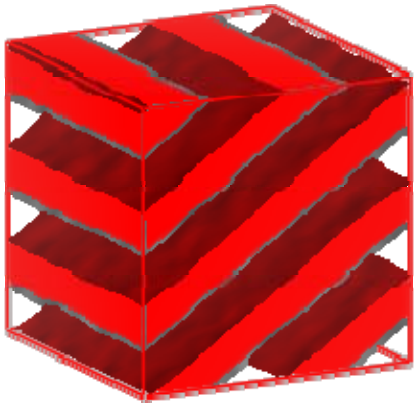

Mesoscale Modeling reproduces main features of the PS/PI phase diagram

Shear Instability of a Gyroid Diblock Copolymer:

validation of mesoscale method

Experiment:

Upon application of shear the gyroid phase of PS/PI copolymer changes to hexagonal phase. Eskimergen et al, Macromolecules (2005) 38, 1286

Mesoscale Modeling:

Mesodyn parametrized using results from lower level multiscale calculations (quantum mechanics and molecular dynamics) for SIBS reproduces this experimental finding. The transition occurs via the perforrated lamella phase

Gyroid phase **Intermediate state** **hexagonal phase (cylinders)**

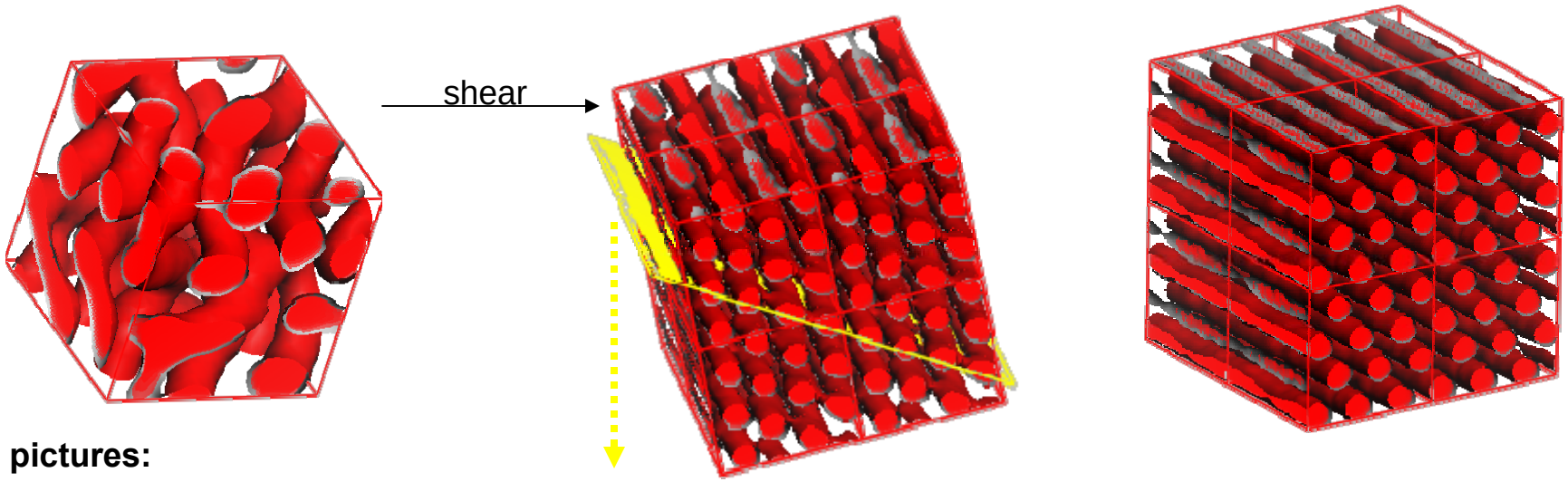

Slice pictures:

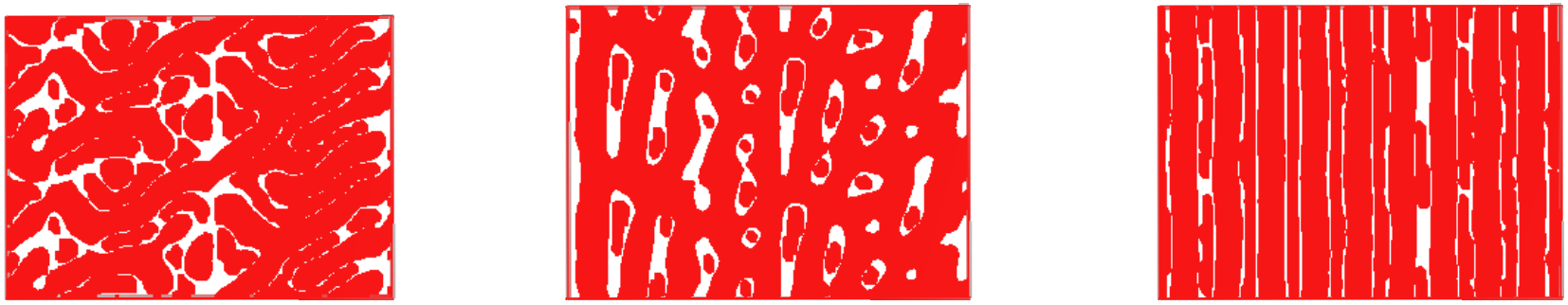

Shear Instability of a BCC Diblock Copolymer

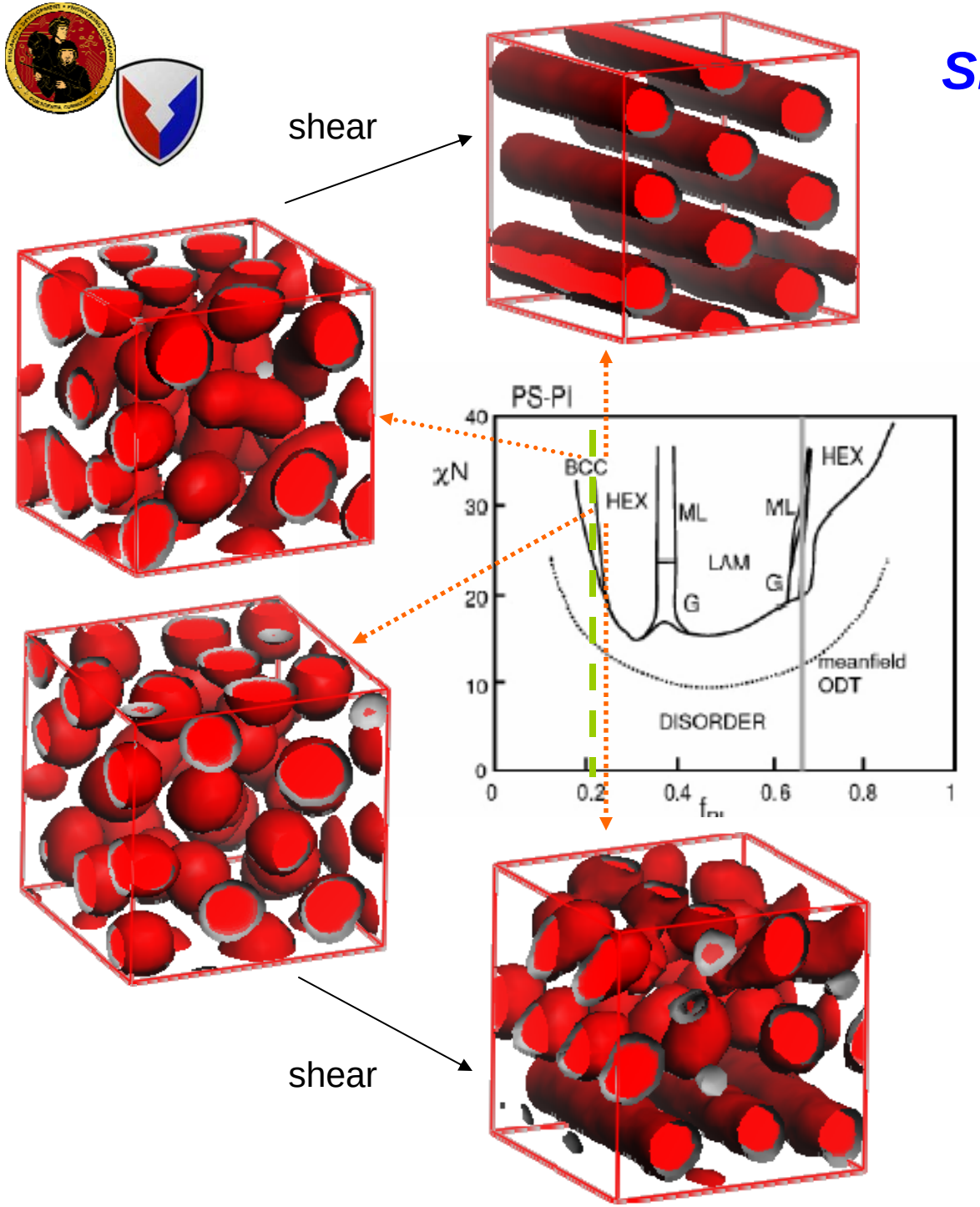

Experiment:
- **Khandpur et al. Macromolecules 28(1995)8796.**
- **Eskimergen et al. Macromolecules 38(2005)1286.**

Modeling:
- **Mesodyn A3B12 (f=0.2)**

Prediction from Mesoscale simulations:

Upon Shear BCC phase transforms into:
- **-hexagonal (for high χN)**
- **-mix of hexagonal & elongated spheres (for low χN)**

Morphology of thin SIBS films with changing surface field

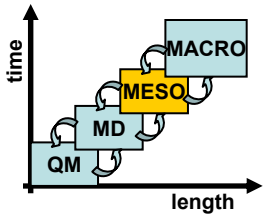

Density fields for polystyrene and polyisobutylene

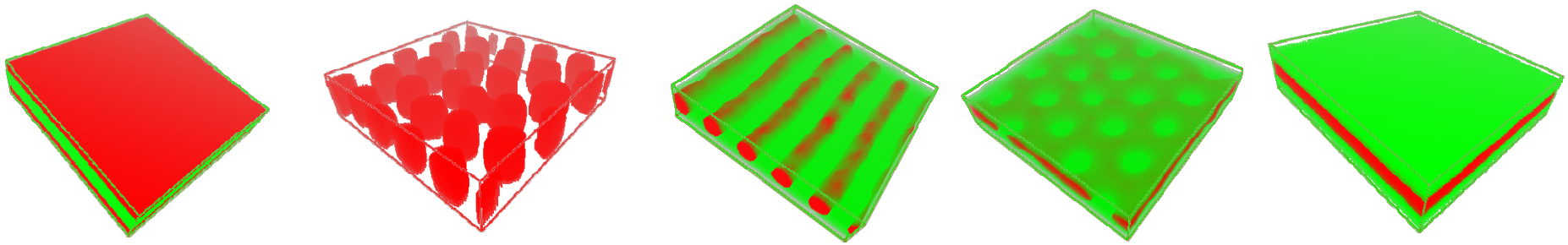

wetting layer | upright cylinders | parallel cylinders | perforated lamella | lamella

Relative (S-IB) Surface field

Cyclohexanol | **cyclohexanone** | **chloroform** | **tetrahydrofuran**

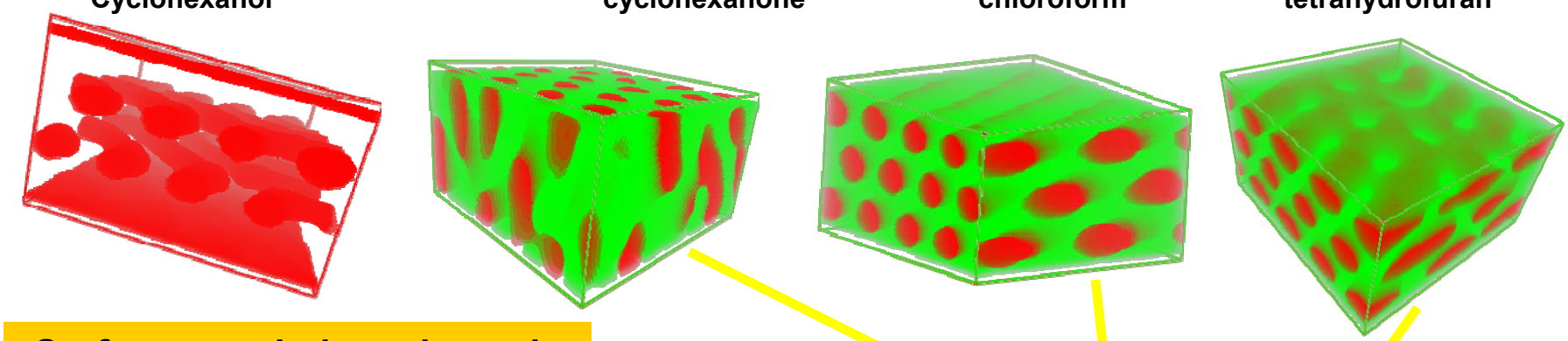

Surface morphology depends on the choice of solvent

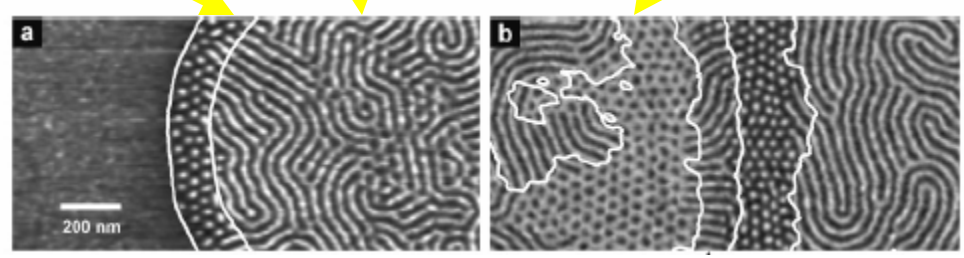

Experiment:
A.Knoll & all., J.Chem.Phys. 120 (2004)1105
Tapping Mode scanning force microscopy
for SBS films on silicon substrate.

Polymer Blends of S-SIBS with Polystyrene (PS)

-Blends of SIBS and up to 40% of PS improve material strength while maintaining elastomeric properties (Antony et al, Polymer Engineering and Science, 43(2003)243)

-What is the nanostructure of such blends in the case of sulfonated, S-SIBS?

Mesoscale prediction:

Blends of S-SIBS and PS form mcrophase separated nanostructures with embedded polystyrene rods which improve strength of polymer

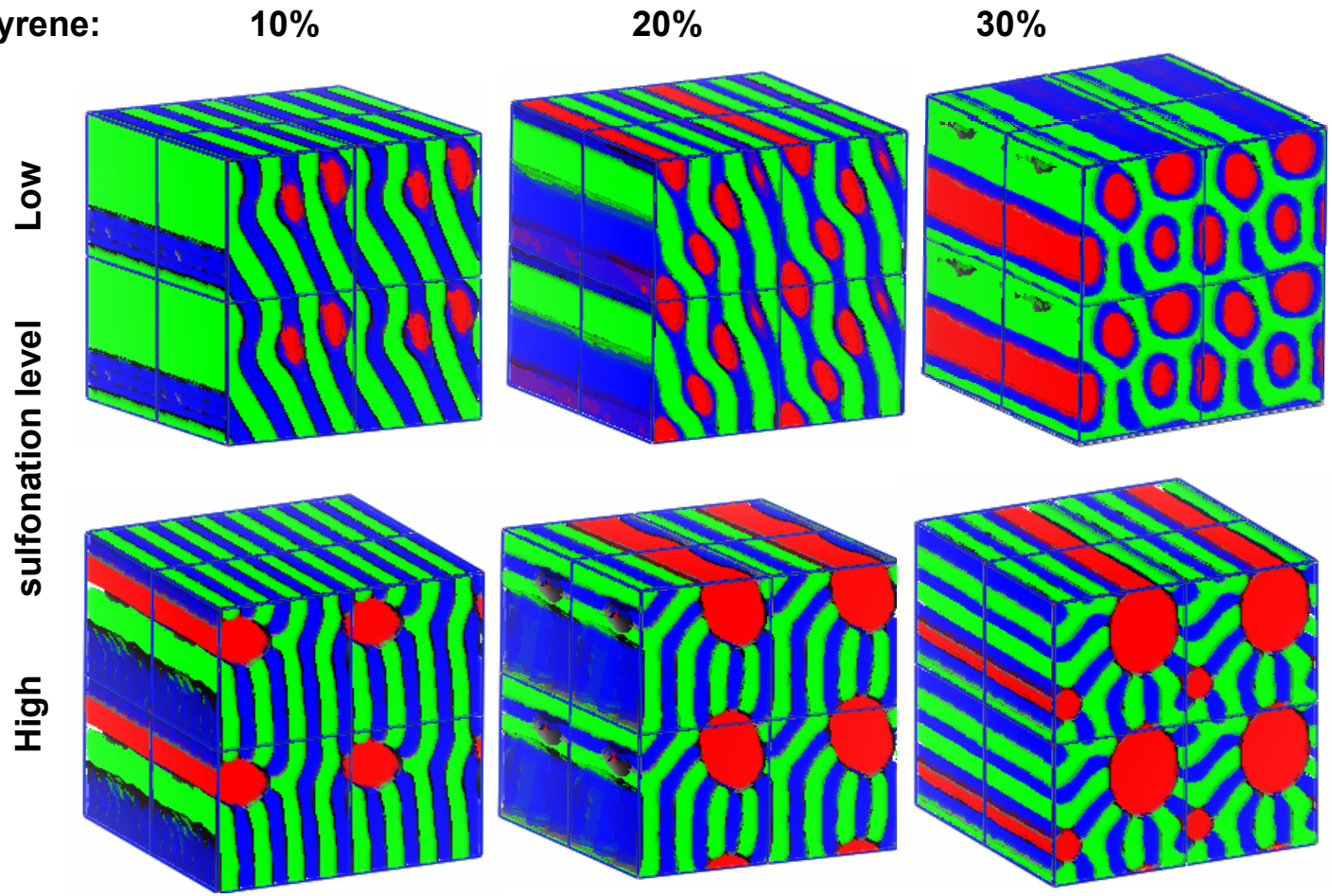

Polymer Blends of S-SIBS with Polyisobutylene (PI)

Content of polyisobutylene: 10% 20% 30%

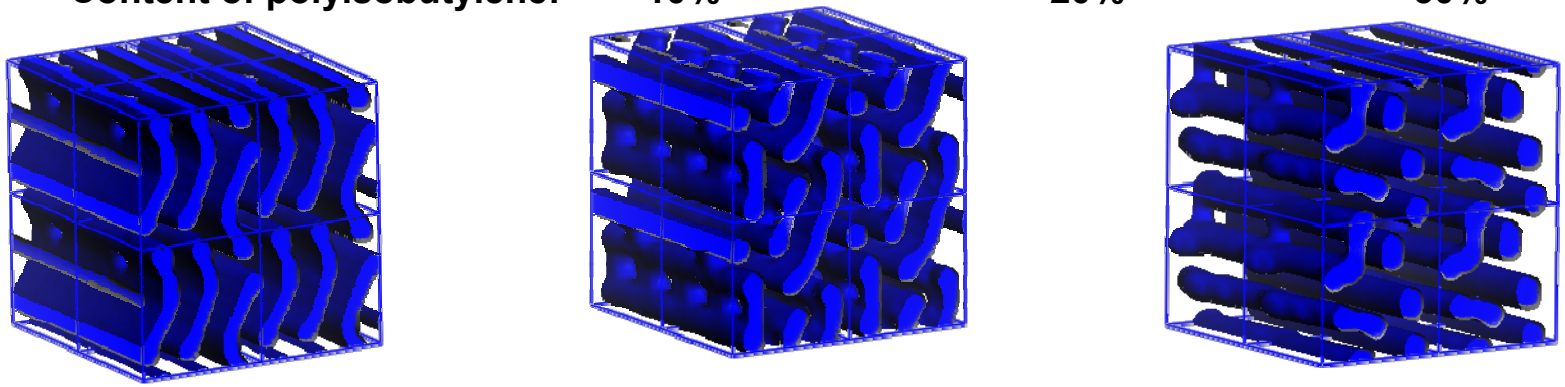

Mesoscale prediction: Blends of S-SIBS and PI form mcrophase separated nanostructures with lamella phase of sulfonated PS broken into perforated lamella sheets and cylinders.

Adding PS makes blend stronger (Young's modulus) while adding PI makes it weaker

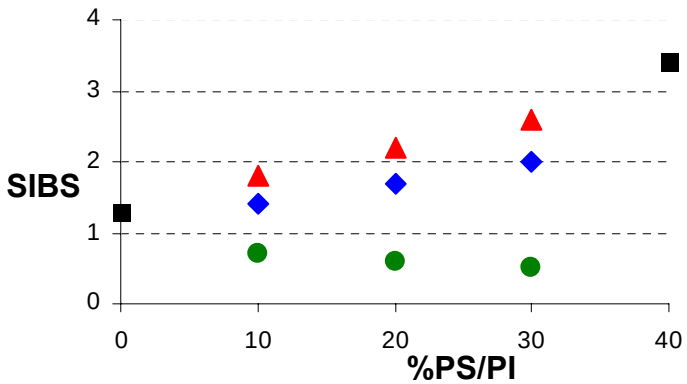

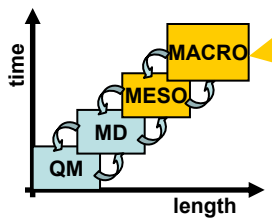

Finite element method based on the mathematical homogenization theory

PS

Increase PS
Low S
High S

Increase PI

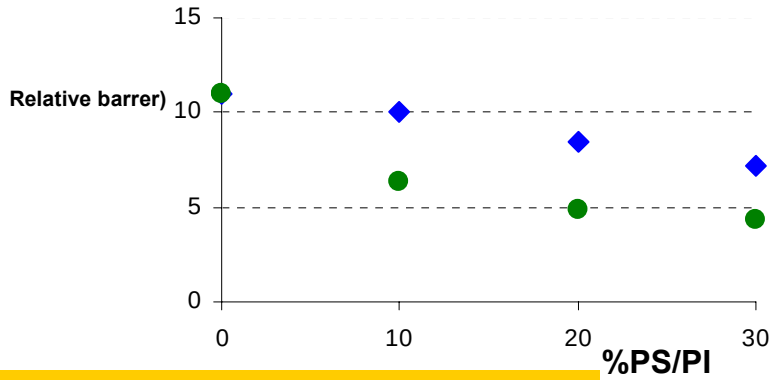

Permeability of water decreases with adding PI and PS

Morphology of thin S-SIBS slabs and nanopores

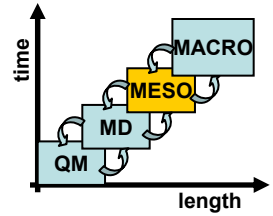

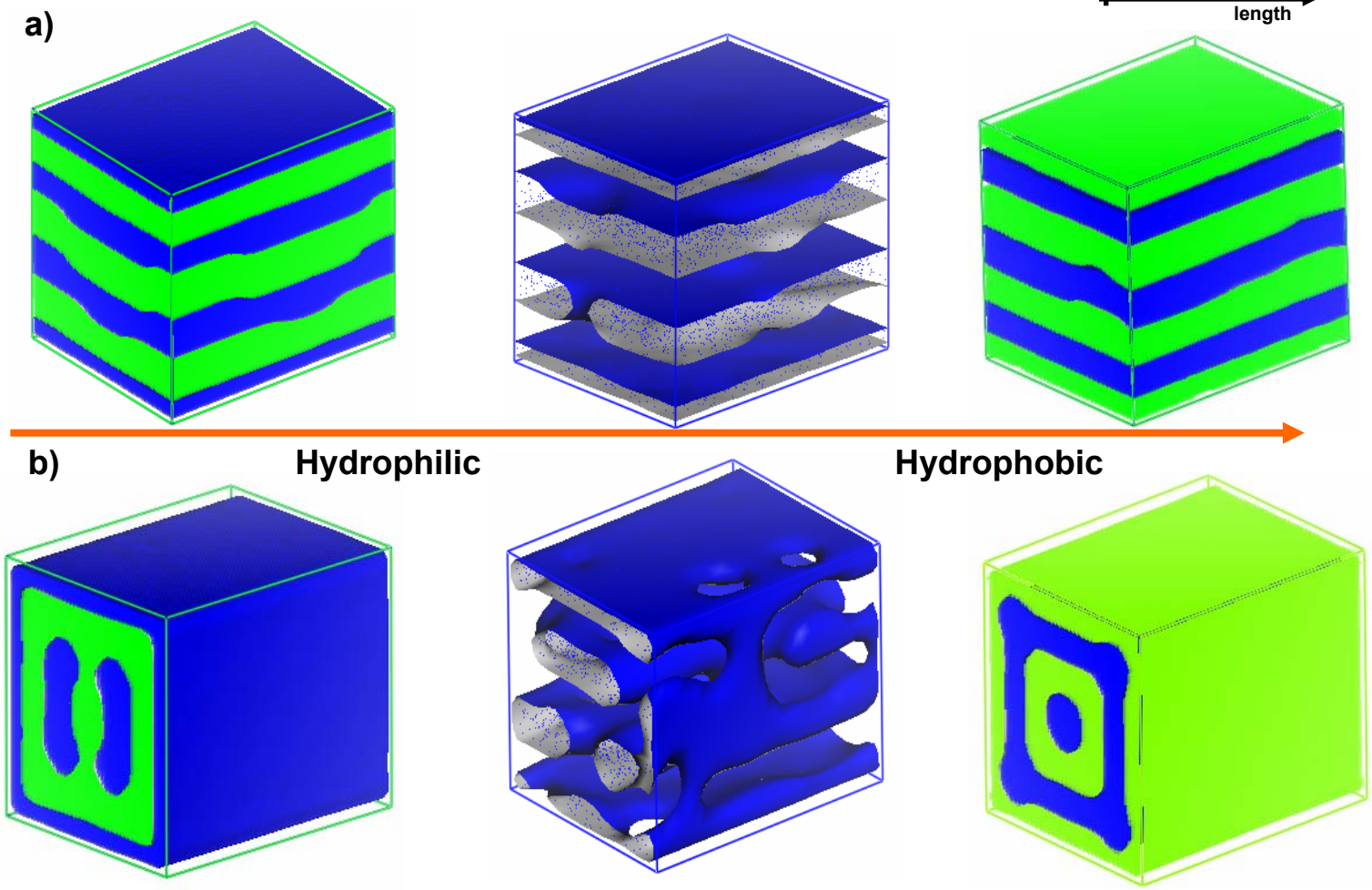

Morphology of SSIBS contained by a) surface, b) nanopore

Mesoscale prediction:

Surface confinement maintains lamellar morphology while nanopores form cylindrical or perforated lamella structures

Metal Cations Improve selectivity

Metal Cations decrease water intake and diffusion:

S-64-SIBS:

	Intake(%)	Diffusion
H^+	308	1.4(-6)
Mg^{++}	73	6.0(-7)
Ca^{++}	62	5.2(-7)
Ba^{++}	28	1.8(-7)

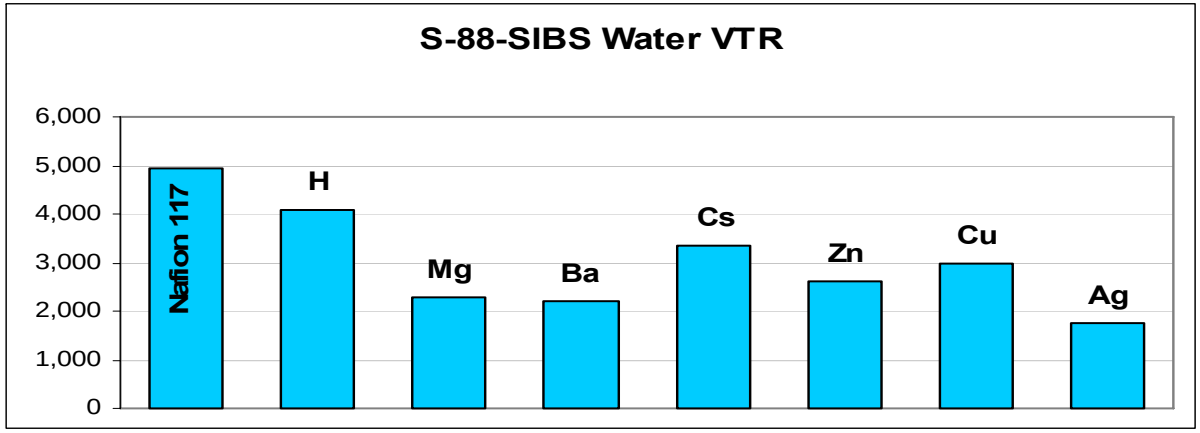

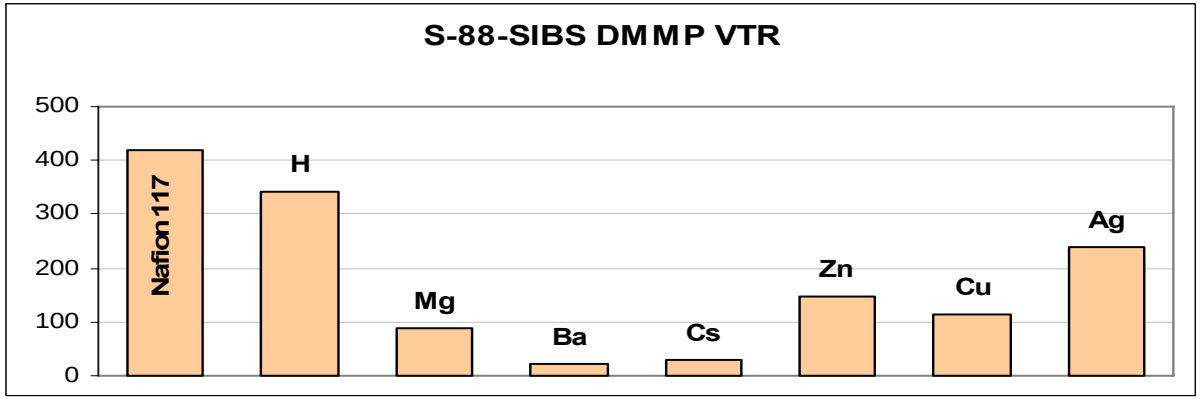

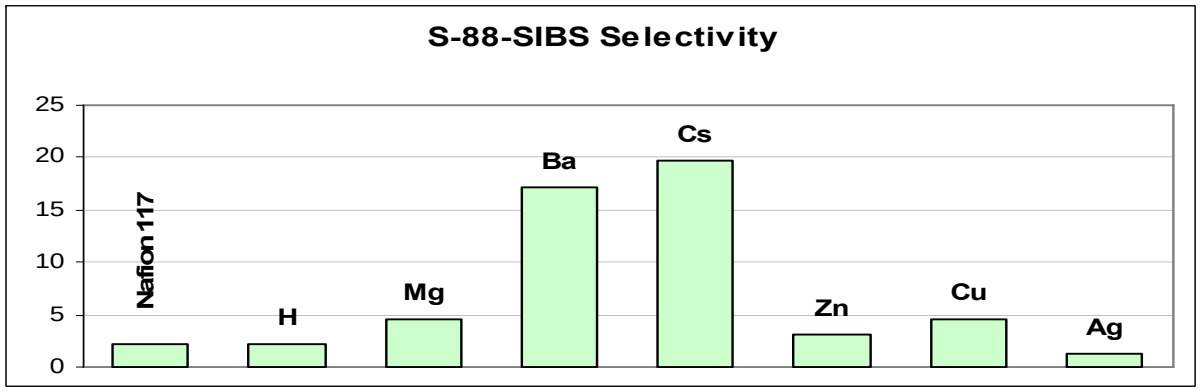

Clusters of Mg^{++} with water and SO_3^-

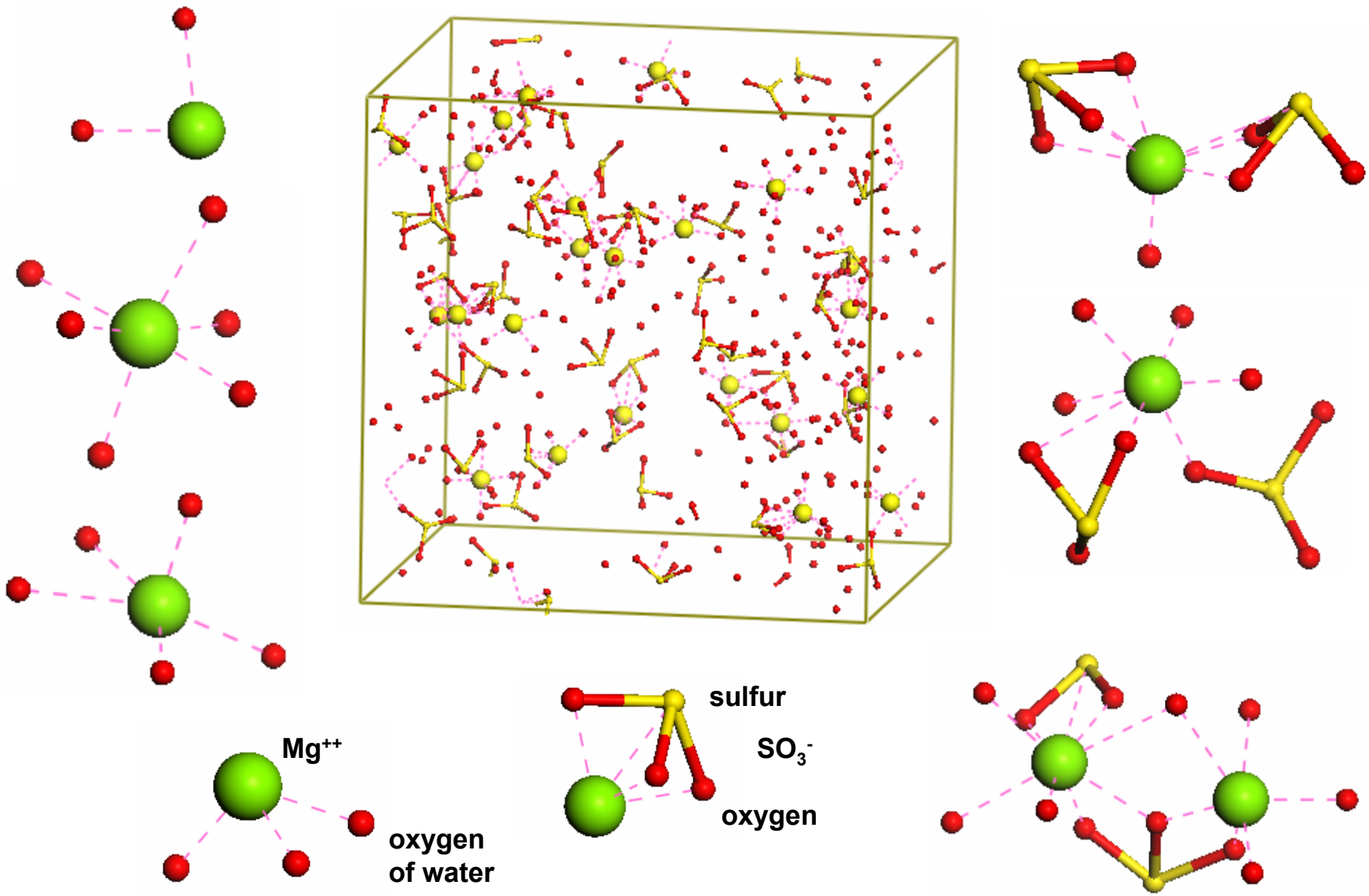

Structure of S-SIBS with metals

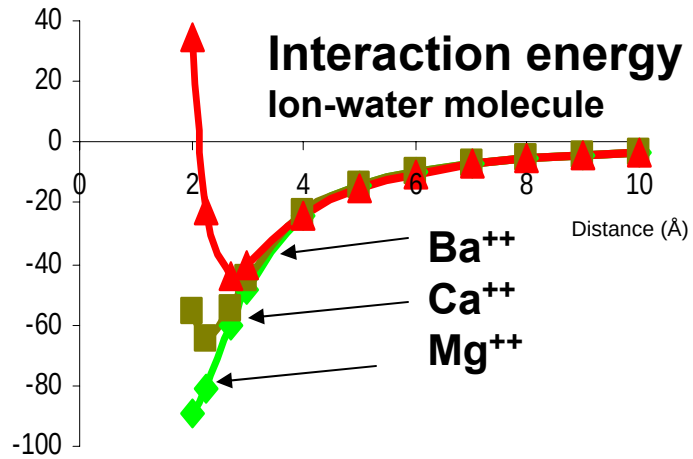

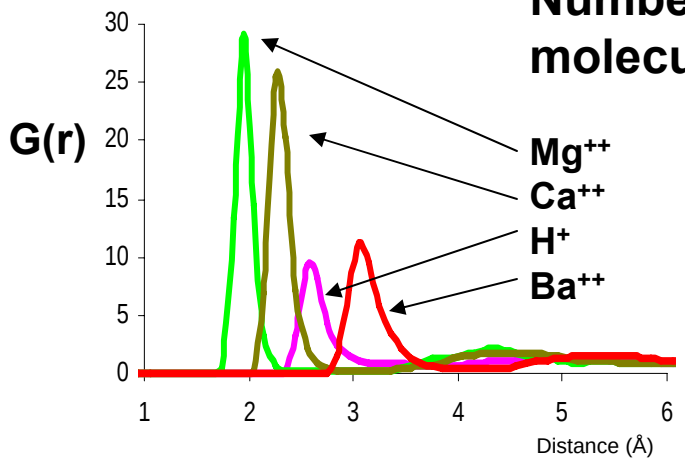

Number of water molecules around ion

	to 1shell	to 4Å
Mg^{++}	4.1	6.1
Ca^{++}	5.4	7.1
H^{+}	3.9	4.3
Ba^{++}	7.4	7.4

Dynamics of cross-linking:

Number of 2- and 3- cross-links of ion-sulfonate group

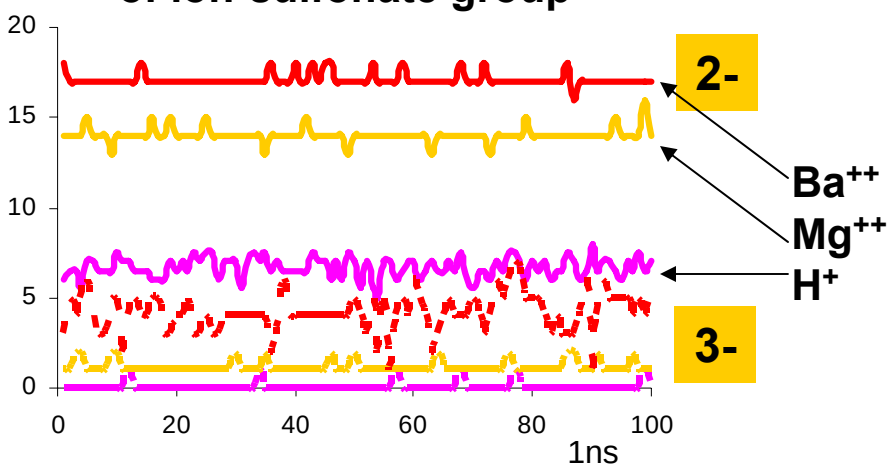

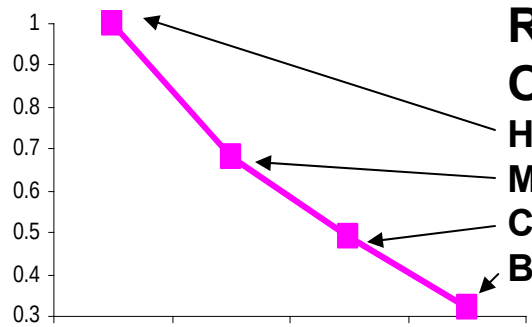

Relative Free/ Occupied space

H^{+}	1
Mg^{++}	0.7
Ca^{++}	0.5
Ba^{++}	0.3

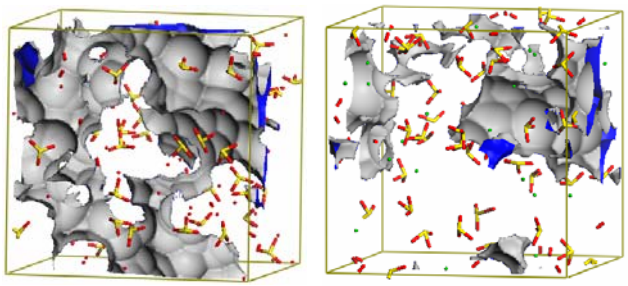

Number of cross-links: Ba>Ca>Mg>H

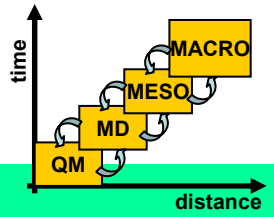

Results from Multiscale Modeling for Permeable Membrane

Understand:

- distribution of water, ions, warfare agents in SIBS bulk and on the surface
- why metal cations slow down water diffusion
- deprotonation of sulfonated group
- how the "percolation" channel looks like and why water flows easily at about 20% sulfonation level

Calculate:

- density of S-SIBS is predicted with accuracy of ~3%
- water self-diffusion follows closely experimental results, if available
- structure (morphology) of a polymer (hexagonal & lamellar)

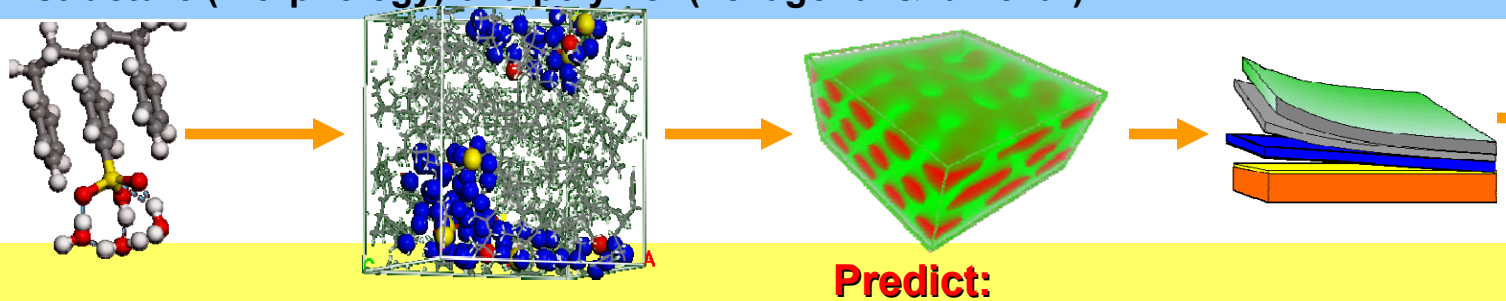

Predict:

- *Blocked* architecture leads to a higher water diffusion coefficient, hence percolation threshold could be achieved at a lower sulfonation level
- Mustard gas & Sarin form stronger than water bonds with surface of polyisobutylene
- *Blocked* architecture enhances selectivity and exhibits a cylindrical morphology
- Morphology of thin (nano) SIBS slabs can be strongly affected by a solvent
- Increasing water concentration leads to spherical micelles of S-SIBS
- Blends of S-SIBS with polystyrene increase mechanical properties but reduce water permeability
- Nanopore confinement leads to cylindrical or perforated lamella morphology
- A new program based on mathematical homogenization theory allows for precise calculation of Young modulus using mesoscale results

Mathematical Homogenization

Solution of an elliptic partial differential equations

$$\frac{\partial}{\partial y} D \frac{\partial \chi}{\partial y} = \frac{\partial D}{\partial y} \qquad \overline{D} = \frac{1}{V}\int_V D\left(1 - \frac{\partial \chi}{\partial y}\right) dV$$

Characteristic Solution for y_{xx}, y_{yy}, y_{zz}…

$$\frac{\sigma_0}{\varepsilon} \le \overline{D} \le \frac{\sigma}{\varepsilon_0}$$

Young Modulus: stress/strain

Palmyra serial and parallel

$$\overline{E} = E_1 V_1 + E_2 V_2 \qquad \frac{1}{\overline{E}} = \frac{V_1}{E_1} + \frac{V_2}{E_2}$$

Norm of Young's modulus tensor:

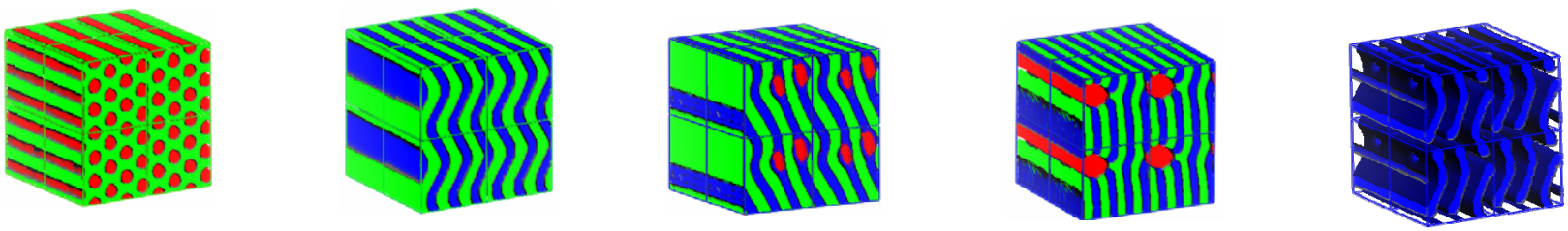

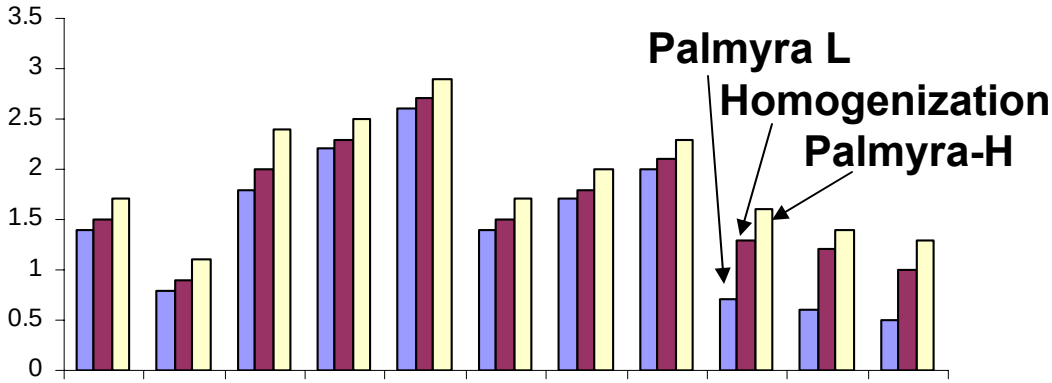

A new accurate approach to calculate mechanical properties

Lamellar Morphology of S-SIBS with water

Change in S-SIBS morphology with water content: from lamellar to micelles

(at 42% sulfonation)
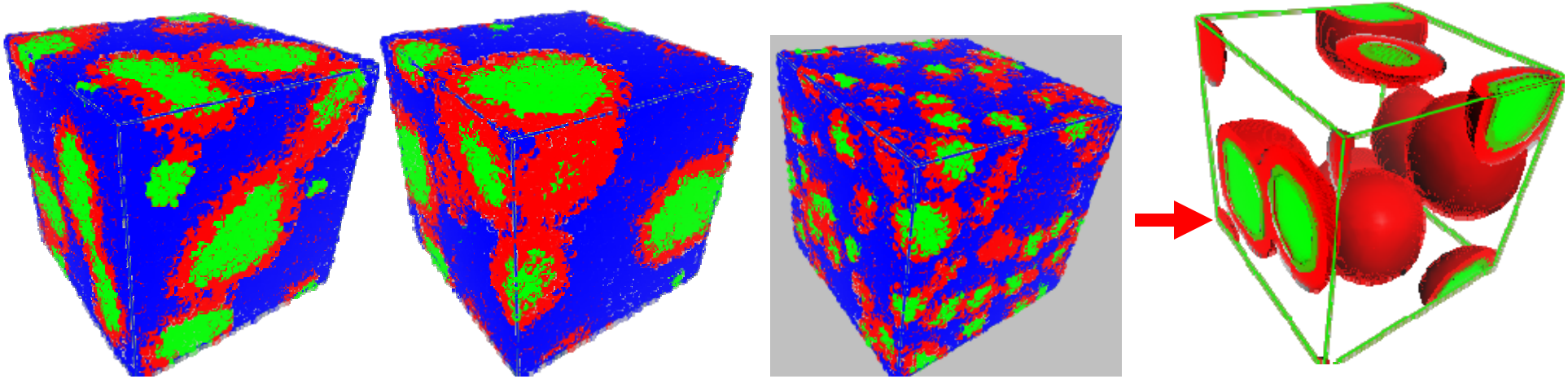
Water (%wt) **60** **70** **80**